Supplementary Information

Synthesis of platinum-containing oligomers utilizing ADMET chemistry and polycondensation of a bisimide with α,ω-dibromoalkanes: examination of triplet–triplet annihilation upconversion

Taichi Sotani,[a] Naoki Shimada,[a] Toshiko Mizokuro,[b] Hiromitsu Sogawa,[a] Kenneth. B. Wagener,[c] Fumio Sanda*[a]

[a] Department of Chemistry and Materials Engineering, Faculty of Chemistry, Materials and Bioengineering, Kansai University, 3-3-35 Yamate-cho, Suita, Osaka 564-8680, Japan. E-mail: sanda@kansai-u.ac.jp

[b] National Institute of Advanced Industrial Science and Technology (AIST), 1-1-1 Higashi, Tsukuba, Ibaraki 305-8565, Japan

[c] Department of Chemistry, University of Florida, PO Box 117200, Gainesville FL 32611, USA

*Corresponding Author. E-mail: sanda@kansai-u.ac.jp.

Experimental section

Measurements

^{1}H (400 MHz), ^{13}C (100 MHz) and ^{31}P NMR (162 MHz) spectra were recorded on JEOL ECS-400 and ECZ-400 spectrometers in $CDCl_3$ and DMSO-d_6 with TMS as an internal standard. IR absorption spectra were measured on a JASCO FT/IR-4100 spectrophotometer. Mass spectra were measured on a Bruker Compact QToF mass spectrometer using an atmospheric pressure chemical ionization (APCI) probe under the following conditions: solvent, THF/*i*-PrOH; mass range (m/z) < 2000; mode, negative. Elemental analysis was performed at the analytical center, Faculty of Engineering, Osaka University. Number-average molecular weight (M_n) and dispersity ($Đ$) values of oligomers were determined by a size exclusion chromatography (SEC) system consisting of JASCO RI-4030, UV-4075, PU4180, DG-2080-53, CO-4060, AS-2055 Plus and LC-Net II/AD, equipped with Shodex polystyrene gel columns KF-805L × 3, using THF as an eluent at a flow rate of 1.0 mL/min, calibrated using polystyrene standards at 40 °C. All absorption and emission spectra were measured in a quartz cell (optical path length: 1 cm). UV–vis absorption spectra were recorded on a JASCO V-630 and V-780 spectrometer. In the polarized case, a Glan-Taylor prism was introduced into the spectrophotometer's optical path. Photoluminescence and excitation spectra were recorded on a Hitachi F-7000 excited at 430 nm. Sample solutions of photoluminescence spectra were stirred for 1 h under N_2 in a glove box to remove dissolved oxygen. Absolute quantum yields of fluorescence and phosphorescence were recorded in a quartz cell on a Hamamatsu Photonics C11347. Fluorescence lifetimes were recorded on a Hamamatsu Photonics C11367-01 excited at 405 nm and monitored at 500 nm. Phosphorescence lifetimes were recorded on a Hamamatsu Photonics C11367-01 excited at 450 nm using a Xe flash lamp (C11567-02, 60 W), monitored at 640 nm, and equipped with a bandpass

filter at 450 nm (Edmund, FWHM: 10 nm, OD4). TTA–UC spectra were measured according to the following procedure: Sample solutions of a sensitizer (c = 5 μM) and 9,10-diphenylanthracene as an emitter (c = 60 μM, Tokyo Chemical Industry Co., D4401) were stirred more than 1 h in a N_2 atmosphere-controlled glove box to remove dissolved oxygen. The UC spectra were recorded using a 450 nm CW laser (450 nm, 4.5 mW, CPS450, THORLABS) as an excitation source on an Ocean photonics FLAME-S equipped with a notch filter at 457 nm. UC emission lifetimes were recorded on a Hamamatsu Photonics C11367-01 excited at 450 nm using a Xe flash lamp (C11567-2, 60 W), monitored at 410 nm, and equipped with an ND filter (5%) and a bandpass filter at 450 nm (Edmund, FWHM: 10 nm, OD4) for excitation light, and a short pass filter at 430 nm (Asahi Spectra, SV0430) for emission. Phosphorescence lifetimes of solutions were recorded in a similar manner to the UC emission lifetimes monitored at 640 nm and equipped with a long pass filter (Optosigma, SCF-50S-48Y). The UC quantum yields were determined using 4-(dicyanomethylene)-2-methyl-6-(4-dimethylaminostyryl)-*4H*-pyran (Φ_F =34% in methanol, Exciton) as a standard in the following equation:

$$\eta_{UC} = 2\Phi_{std}\left(\frac{A_{std}}{A_{unk}}\right)\left(\frac{I_{unk}}{I_{std}}\right)\left(\frac{\eta_{unk}}{\eta_{std}}\right)^2$$

where Φ_{std} is the quantum yield of fluorescence of the standard, η_{UC}, A_{unk}, I_{unk} and η_{unk} represent the quantum efficiency, absorbance, integrated photoluminescence intensity and refractive index of the sample. The terms for the subscript std represent the reference values.[S1] The emission spectra of the films were recorded in a flow cell on the Ocean

photonics FLAME-S equipped with the notch filter using the 450 nm CW laser as the excitation source. TGA was measured on a SHIMADZU thermogravimetric analyzer TGA-50. DSC was measured on a SEIKO DSC 6200 differential scanning calorimeter under N_2. XRD was measured on a Rigaku Smart Lab. X-ray diffractometer (CuKα1 for X-ray source).

Materials

All solvents for the reaction were degassed by Ar bubbling and desiccated with molecular sieve 4A. All other reagents were commercially obtained and used as received without purification.

Synthesis of monomer 1

4-Bromo-1,8-naphthalimide[S2]

To a dispersion of 4-bromo-1,8-naphthalic anhydride (8.31 g, 30.0 mmol) in ethanol (240 mL), 30% aqueous ammonia (60 mL) was added. The resulting mixture was heated with refluxing overnight. After cooling the resulting solution, the solid was filtered, washed with ethanol, and dried to obtain the title compound as a beige solid (7.18 g, 26.0 mmol) in 87% yield. ^{1}H NMR (400 MHz, DMSO-d_6): δ 7.93–8.05 (Ar, 1H), 8.16–8.34 (Ar, 1H), 8.44–8.55 (Ar, 1H), 11.87 (s, 1H, NH) ppm.

***N*-(5-Hexenyl)-4-bromo-1,8-naphthalimide**

A mixture of 4-bromo-1,8-naphthalimide (1.38 g, 5.0 mmol), 6-bromo-1-hexene (0.82 g, 5.0 mmol), K_2CO_3 (0.97 g, 7.0 mmol) and DMF (10.0 mL) was stirred at 90 °C overnight,

then concentrated to obtain a brown solid. It was purified by silica gel column chromatography eluted with $CHCl_3$ to obtain the title compound as slightly a yellow solid (1.59 g) in 88% yield. ^{1}H NMR (400 MHz, $CDCl_3$): δ 1.51–1.57 (m, 2H, –CH_2–), 1.71–1.81 (m, 2H, –CH_2–), 2.10–2.18 (m, 2H, –CH_2–CH=), 4.15–4.20 (m, 2H, –NCH_2-), 4.93–5.04 (m, 2H, =CH_2), 5.76–5.87 (m, 1H, –CH=), 7.82–7.87 (1H, Ar), 8.04 (1H, Ar), 8.42 (1H, Ar), 8.56–8.58 (1H, Ar), 8.63–8.67 (1H, Ar) ppm. ^{13}C NMR (100 MHz, $CDCl_3$): δ 26.3, 27.5, 33.4, 40.4, 114.7, 122.2, 123.0, 128.0, 128.9, 130.2, 130.5, 131.0, 131.2, 132.0, 133.2, 138.5, 163.5 ppm.

_N_-(5-Hexenyl)-4-[2-(trimethylsilyl)ethynyl]-1,8-naphthalimide

_N_-(5-Hexenyl)-4-bromo-1,8-naphthalimide (1.43 g, 4.0 mmol), $PdCl_2(PPh_3)_2$ (28.1 mg, 0.04 mmol), CuI (7.6 mg, 0.04 mmol) and 2-(dicyclohexylphosphino)-2',4',6'-triisopropyl-1,1'-biphenyl (XPhos, 19.1 mg, 0.04 mmol) were dissolved in a solution of THF (4 mL) and Et_3N (1 mL) under Ar. Trimethylsilylacetylene (TMSA, 0.59 g, 0.85 mL, 6.0 mmol) was added to the resulting mixture, and heated with refluxing overnight. CH_2Cl_2 (50 mL) was added to the mixture, and the mixture was washed with 1.0 M NH_4Cl aq. The organic layer was separated from the water layer, dried over anhydrous $MgSO_4$, and concentrated. The residual mass was purified by silica gel column chromatography eluted with CH_2Cl_2 to obtain the title compound as a yellow solid (1.49 g, 3.9 mmol) quantitatively. ^{1}H NMR (400 MHz, $CDCl_3$): δ 0.35 (s, 9H, –$Si(CH_3)_3$), 1.49–1.57 (m, 2H, –CH_2–), 1.71–1.79 (m, 2H, –CH_2–), 2.10–2.17 (m, 2H, –CH_2–CH=), 4.18 (t, J = 7.5 Hz, 2H, –NCH_2–), 4.93–5.04 (m, 2H, =CH_2), 5.77–5.87 (m, 1H, –CH=), 7.80−7.84 (1H, Ar), 7.88−7.90 (1H, Ar), 8.50−8.52 (1H, Ar), 8.62−8.64 (2H, Ar) ppm. ^{13}C NMR (100 MHz, $CDCl_3$): δ –0.2, 26.4, 27.6, 33.5, 40.3, 101.2, 105.2, 114.7, 122.3, 122.9, 127.2, 127.5, 127.9, 130.2, 131.1, 131.5, 131.7, 132.3, 138.5, 163.6, 163.9 ppm.

_N_-(5-Hexenyl)-4-ethynyl-1,8-naphthalimide

_N_-(5-Hexene-1-yl)-4-[2-(trimethylsilyl)ethynyl]-1,8-naphthalimide (1.69 g, 4.5 mmol) and K_2CO_3 (1.24 g, 9.0 mmol) were added to a solution of CH_2Cl_2 (5 mL) and CH_3OH (5 mL). The resulting mixture was stirred at r.t. for 30 min. CH_2Cl_2 (30 mL) was added to the mixture, and the resulting mixture was washed with saturated NaCl aq. The organic layer was separated from the water layer, dried over anhydrous $MgSO_4$, concentrated, and the residual mass was purified by silica gel column chromatography eluted with CH_2Cl_2 to obtain a yellow solid (1.22 g). It was washed with warm hexane and the insoluble parts were removed by filtration. The filtrate was concentrated to obtain the title compound as a yellow solid (1.16 g, 3.8 mmol) in 85% yield. ^{1}H NMR (400 MHz, $CDCl_3$): δ 1.51–1.57 (m, 2H, –CH_2–), 1.72–1.81 (m, 2H, –CH_2–), 2.11–2.17 (m, 2H, –CH_2–CH=), 3.74 (s, 1H, C≡CH), 4.18 (t, J = 7.5 Hz, 2H, –NCH_2–), 4.93–5.05 (m, 2H, =CH_2), 5.77–5.87 (m, 1H, –CH=), 7.81–7.85 (1H, Ar), 7.93–7.96 (1H, Ar), 8.52–8.54 (1H, Ar), 8.61–8.68 (2H, Ar) ppm. ^{13}C NMR (100 MHz, $CDCl_3$): δ 26.4, 27.6, 33.5, 40.3, 80.3, 86.5, 114.7, 122.7, 122.9, 126.1, 127.6, 127.8, 130.1, 131.6, 131.6, 131.8, 132.1, 138.5, 163.5, 163.8 ppm. IR (KBr): 3568, 3227, 3078, 2939, 2855, 2098, 1696, 1656, 1613, 1587, 1508, 1465, 1441, 1389, 1354, 1322, 1286, 1245, 1174, 1115, 1094, 1074, 1061, 1010, 995, 954, 913, 864, 806, 783, 753, 737, 695, 670, 615, 680, 504 cm^{-1}.

Monomer 1

Compound **9** (913 mg, 3.00 mmol), $PtI_2(PEt_3)_2$ (822.3 mg, 1.20 mmol) and CuI (57.1 mg, 0.30 mmol) were dissolved a solution of CH_2Cl_2 (5 mL) and Et_3N (5 mL) under Ar. The resulting mixture was stirred at r.t. overnight. CH_2Cl_2 (50 mL) was added to the mixture, and the solution was washed with 1.0 M NH_4Cl aq. The organic layer was dried over

anhydrous $MgSO_4$, and concentrated. The residual mass was purified by silica gel column chromatography eluted with CH_2Cl_2 → $CH_2Cl_2/CH_3COOC_2H_5$ = 100/1 to obtain **1** as yellow solid (1.21 g, 1.16 mmol). Yield = 97%. ^{1}H NMR (400 MHz, $CDCl_3$): δ 1.23–1.31 (m, 18H, –CH_3), 1.49–1.57 (m, 4H, –CH_2–), 1.72–1.79 (m, 4H, –CH_2–), 2.10–2.24 (m, 16H, –PCH_2–, –CH_2–CH=), 4.15–4.20 (m, 4H, –NCH_2–), 4.93–5.04 (m, 4H, =CH_2), 5.77–5.87 (m, 2H, –CH=), 7.65–7.67 (2H, Ar), 7.71–7.75 (2H, Ar), 8.46–8.48 (2H, Ar), 8.58–8.60 (2H, Ar), 8.77–8.79 (2H, Ar) ppm. ^{13}C NMR (100 MHz, $CDCl_3$): δ 8.4, 16.4, 16.6, 16.8, 26.4, 27.6, 33.5, 40.2, 108.9, 114.6, 118.7, 122.8, 126.2, 128.5, 128.9, 131.1, 132.1, 133.2, 133.4, 138.6, 164.2, 164.5 ppm. ^{31}P NMR (162 MHz, $CDCl_3$): δ 13.0 (J = 2330 Hz) ppm. IR (KBr): 3076, 2960, 2934, 2876, 2084, 1695, 1658, 1610, 1581, 1506, 1458, 1438, 1421, 1383,1351, 1238, 1170, 1145, 1093, 1067, 1037, 994, 914, 864, 789, 762, 734, 714, 643, 592, 581, 519 cm^{-1}. APCI-MS (m/z): calcd. 1035.3838 ($[C_{52}H_{62}N_2O_4P_2Pt]^-$), found 1035.3833. Anal. Calcd. for $C_{52}H_{62}N_2O_4P_2Pt$: C 60.28, H 6.03, N 2.70. Found: C 60.28, H 6.18, N 2.74.

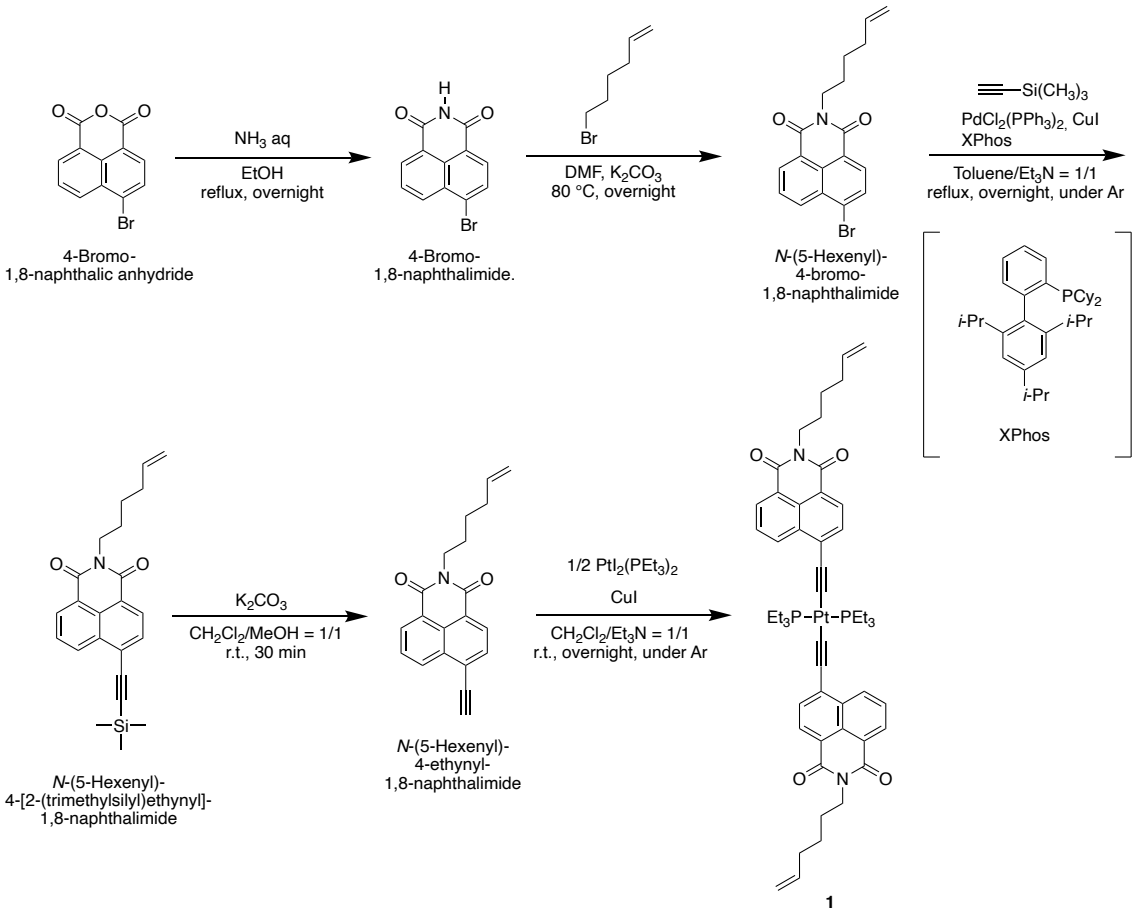

Scheme S1 Synthetic route for monomer **1**.

Synthesis of monomer 2

4-[2-(Trimethylsilyl)ethynyl]-1,8-naphthalimide. 4-Bromo-1,8-naphthalic anhydride (3.31 g, 12.0 mmol), $PdCl_2(PPh_3)_2$ (84.2 mg, 0.12 mmol), CuI (22.9 mg, 0.12 mmol) and XPhos (57.2 mg, 0.12 mmol) were dissolved in a solution of DMF (15 mL) and Et_3N (15 mL) under Ar. TMSA (1.47 g, 2.10 mL, 15.0 mmol) was added to the solution, and the resulting mixture was heated at 80 °C overnight. CH_2Cl_2 (70 mL) was added to the mixture, and the solution was washed with 1.0 M NH_4Cl aq. The organic layer was separated from the water layer, dried over anhydrous $MgSO_4$, and concentrated. The residual mass was purified by silica gel column chromatography eluted with CH_2Cl_2 → $CH_2Cl_2/CH_3COOC_2H_5$ = 20/1 to obtain the title compound as a yellow solid (2.86 g, 9.7

mmol) in 81% yield. ^{1}H NMR (400 MHz, DMSO-d_6): δ 0.36 (s, 9H, –Si(CH_3)$_3$), 7.95–8.03 (2H, Ar), 8.34–8.40 (1H, Ar), 8.47–8.52 (1H, Ar), 8.55–8.62 (1H, Ar), 11.81 (s, 1H, NH) ppm. ^{13}C NMR (100 MHz, DMSO-d_6): δ –0.3, 101.2, 104.7, 122.7, 123.0, 125.7, 128.2, 128.4, 129.1, 130.4, 131.2, 131.4, 163.4, 163.8 ppm.

4-Ethynyl-1,8-naphthalimide

4-[2-(Trimethylsilyl)ethynyl]-1,8-naphthalimide (1.33 g, 6.0 mmol) was added to a solution of THF (20 mL) and MeOH (20 mL). KOH aq (10 mL, 1.01 g, 18.0 mmol) was added to the solution, and the resulting mixture was stirred at r.t. for 2 h. The solution was acidified with 1.0 M HCl aq. to precipitate a solid mass. It was collected by filtration, and the solid was washed with water and cooled MeOH to obtain a yellow solid (1.08 g, 4.9 mmol) in 81% yield. ^{1}H NMR (400 MHz, DMSO-d_6): δ 5.09 (s, 1H, C≡CH), 7.96–8.05 (2H, Ar), 8.39–8.41 (1H, Ar), 8.50–8.52 (1H, Ar), 8.62–8.64 (1H, Ar), 11.83 (s, 1H, NH) ppm.

Monomer 2

4-Ethynyl-1,8-naphthalimide (663.7 mg, 3.0 mmol), $PtI_2(PEt_3)_2$ (1.08 g, 1.5 mmol) and CuI (57.1 mg, 0.30 mmol) were dissolved a solution of DMF (10 mL) and Et_3N (10 mL) under Ar. The resulting mixture was stirred at r.t. for 3 days to precipitate a solid. The resulting mixture was added to a solution of 1.0 M NH_4Cl aq (100 mL) and MeOH (100 mL), and stirred at r.t. overnight to precipitate a solid mass. It was collected by filtration and washed with water and MeOH, and dried *in vacuo* to obtain yellow solid. It was purified by silica gel chromatography eluted with CH_2Cl_2 → CH_2Cl_2/MeOH = 20/1 to obtain **2** as a yellow solid (1.21 g, 1.39 mmol) in 92% yield. ^{1}H NMR (400 MHz, DMSO-d_6): δ 1.18–1.26 (m, 18H, –CH_3), 2.17–2.21 (m, 12H, –PCH_2–), 7.69 (2H, Ar), 7.90 (2H,

Ar), 8.33 (2H, Ar), 8.45 (2H, Ar), 8.73 (2H, Ar), 11.66 (s, 2H, NH) ppm. ^{31}P NMR (162 MHz, DMSO-d_6): δ 13.9 (J = 2279 Hz) ppm. IR (KBr): 3648, 3175, 3059, 2962, 2931, 2077, 1693, 1674, 1579, 1505, 1458, 1391, 1363, 1265, 1235, 1188, 1102, 1039, 989, 856, 779, 758, 698, 640, 606, 519 cm^{-1}. APCI-MS (m/z): calcd. 871.2268 ([$C_{40}H_{42}N_2O_4P_2Pt$]$^-$), found 871.2256.

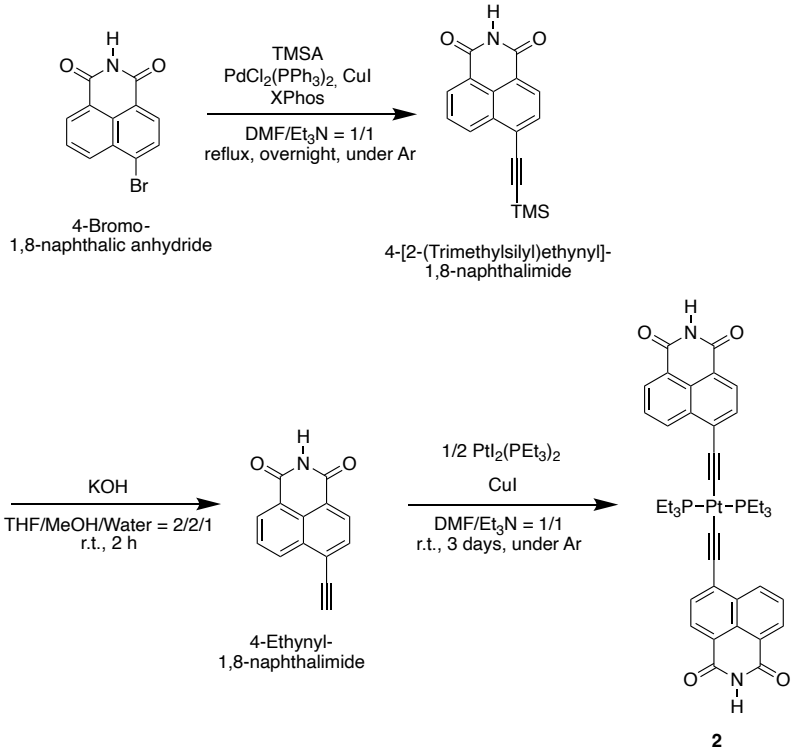

Scheme S2 Synthetic route for monomer **2**.

ADMET oligomerization

A solution of 1,3-bis(2,4,6-trimethylphenyl)-2-imidazolidinylidene)dichloro(phenylmethylene)(tricyclohexylphosphine)ruthenium (Grubbs second generation catalyst, **G2**, 5.10 mg, 0.006 mmol) in *o*-dichlorobenzene (1.2 mL) was added to monomer **1** (310.8 mg, 0.03 mmol) fed in a Schlenk tube connected

with a trap, a mercury manometer and a diaphragm vacuum pump, in that order as shown in Fig. S1. The solution was degassed by the freeze-pump-thaw method three times. It was stirred at 50 °C for 48 h under reduced pressure (11.2 kPa) using a KNF diaphragm vacuum pump N810.3FT.18(Ex). Ethyl vinyl ether (1.0 mL, ca. 0.01 mol) and CH_2Cl_2 (1.0 mL) were added to the solution, and stirred at r.t. for 15 min. The resulting mixture was poured into a large amount of MeOH to precipitate a solid mass. It was separated by filtration using a membrane filter (ADVANTEC H100A047A), washed with large amount of MeOH, and dried *in vacuo* to obtain a solid mass. It was dissolved in CH_2Cl_2, and reprecipitated with hexane to obtain oligo(**1**) as a yellow solid in 96% yield. M_n = 8,900, $Đ$ = 2.21.

Fig. S1 Photograph of an apparatus for ADMET oligomerization.

Polycondensation of 2 with 3a–3c

Typical procedure: A solution of **2** (261.5 mg, 0.30 mmol) in *N*-methylpyrrolidone (NMP) (14.4 mL) was heated at 90 °C until **2** was completely dissolved in a Schlenk tube. K_2CO_3 (414.6 mg, 3.0 mmol) and a solution of 1,6-dibromohexane (**3a**, 0.6 mL, 73.2 mg, 0.30 mmol) were added to the solution, and the mixture was stirred at 90 °C for 6 h. It was poured into a large amount of MeOH (300 mL) to precipitate a solid. It was separated

by filtration using a membrane filter (ADVANTEC H100A047A), washed with large amount of water and MeOH, and dried *in vacuo* to obtain oligo(**2-3a**) in 94% yield. Oligo(**2-3b**) and oligo(**2-3c**) were synthesized in a manner similar to oligo(**2-3a**).

Spectroscopic data for the oligomers

Oligo(**1**): Yield 96%. ^{1}H NMR (400 MHz, $CDCl_3$): δ 1.16–1.31 (m, 18H, –CH_3), 1.41–1.88 (m, 12H, –CH_2–), 2.04–2.42 (m, 16H, –PCH_2–, –CH_2–CH=), 4.15–4.35 (m, 4H, –NCH_2–), 4.93–5.11 (m, 1H, =CH_2), 5.36–5.58 (internal –CH=), 5.77–5.92 (terminal –CH=), 7.61–7.74 (4H, Ar), 8.46–8.60 (4H, Ar), 8.76–8.78 (2H, Ar) ppm. ^{31}P NMR (162 MHz, $CDCl_3$): δ 13.0 (J = 2330 Hz) ppm. Oligo(**2-3a**): Yield 94%. ^{1}H NMR (400 MHz, $CDCl_3$): δ 1.19–1.31 (m, 18H, –CH_3), 1.43–1.76 (m, 8H), 2.10–2.22 (m, 12H, –PCH_2–), 4.18 (t, J = 7.5 Hz, 4H, –NCH_2–), 7.60–7.77 (4H, Ar), 8.37–8.47 (2H, Ar), 8.52–8.59 (2H, Ar), 8.76–8.83 (2H, Ar) ppm. ^{31}P NMR (162 MHz, $CDCl_3$): δ 13.0 (J = 2355 Hz) ppm. Oligo(**2-3b**): Yield 93%. ^{1}H NMR (400 MHz, $CDCl_3$): δ 1.19–1.31, 1.43–1.76 (m, 30H, –CH_3, –CH_2–), 2.10–2.22 (m, 12H, –PCH_2–), 4.18 (t, J = 7.5 Hz, 4H, –NCH_2–), 7.60–7.77 (4H, Ar), 8.37–8.47 (2H, Ar), 8.52–8.59 (2H, Ar), 8.76–8.83 (2H, Ar) ppm. ^{31}P NMR (162 MHz, $CDCl_3$): δ 13.0 (J = 2355 Hz) ppm. Oligo(**2-3c**): Yield 92%. ^{1}H NMR (400 MHz, $CDCl_3$): δ 1.09–1.41, 1.63–1.74 (m, 38H, –CH_3, –CH_2–), 2.16–2.23 (m, 12H, –PCH_2–), 4.17 (t, J = 7.5 Hz, 4H, –NCH_2–), 7.63–7.76 (4H, Ar), 8.44–8.48 (2H, Ar), 8.56–8.60 (2H, Ar), 8.74–8.80 (2H, Ar) ppm. ^{31}P NMR (162 MHz, $CDCl_3$): δ 13.0 (J = 2355 Hz) ppm.

Computations

All computational calculations were performed with the Gaussian 16 program,[S3] Fujitsu-Arm-G16 Rev C.01 running on Fugaku, Center for Computational Science, RIKEN, and ES64L-G16 Rev B.01 running on the supercomputer systems, Academic Center for Computing and Media Studies, Kyoto University. The UV–vis and IR absorption spectra were simulated by the TD-DFT and DFT methods with the ωB97XD functional in conjugation with the basis set, 6-31G* (C, H, N, O, P) and LANL2DZ (Pt).

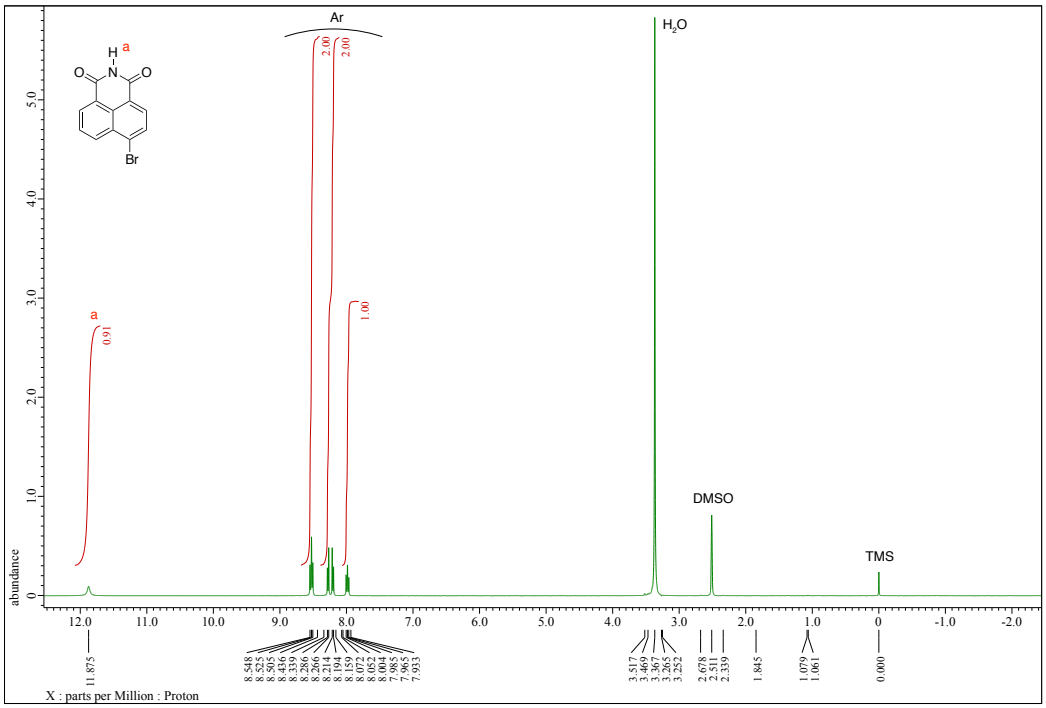

Fig. S2 ^{1}H-NMR (400 MHz) spectrum of 4-bromo-1,8-naphthalimide measured in DMSO-d_6 with tetramethylsilane (TMS) as an internal standard.

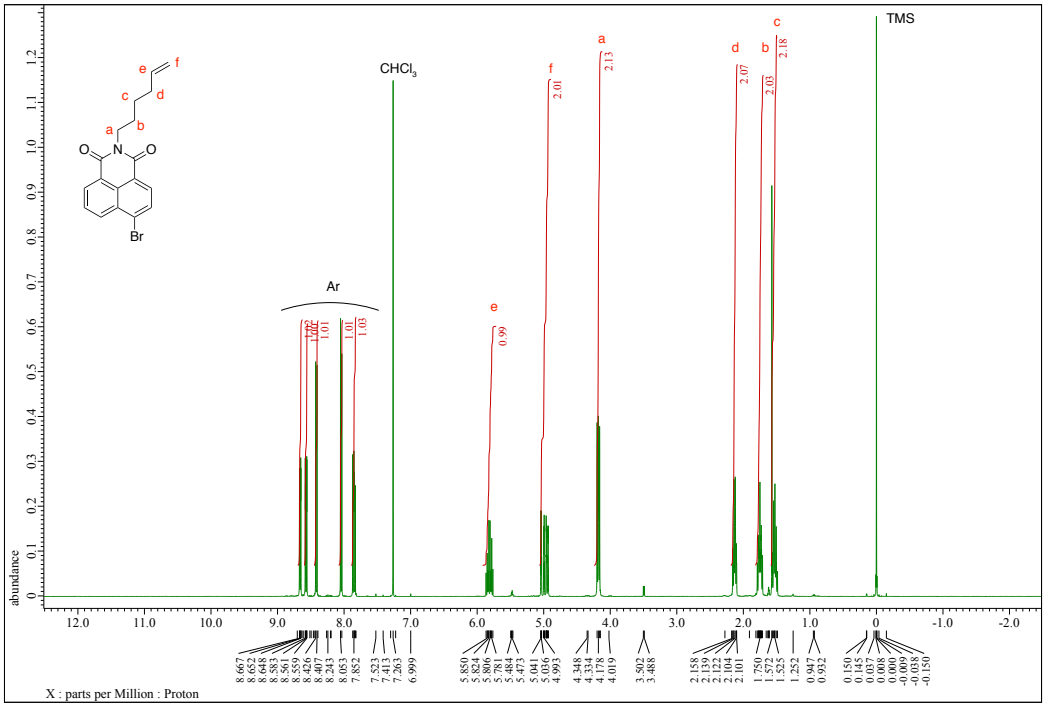

Fig. S3. ^{1}H-NMR (400 MHz) spectrum of *N*-(5-hexenyl)-4-bromo-1,8-naphthalimide measured in $CDCl_3$ with TMS as an internal standard.

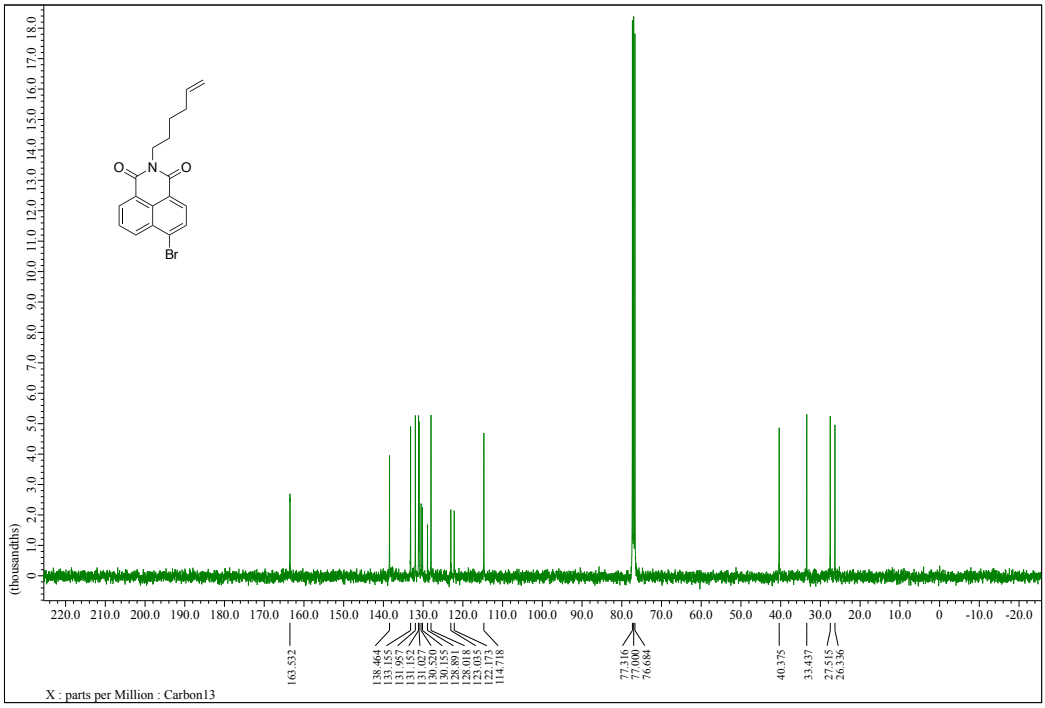

Fig. S4. ^{13}C-NMR (100 MHz) spectrum of *N*-(5-hexenyl)-4-bromo-1,8-naphthalimide measured in $CDCl_3$.

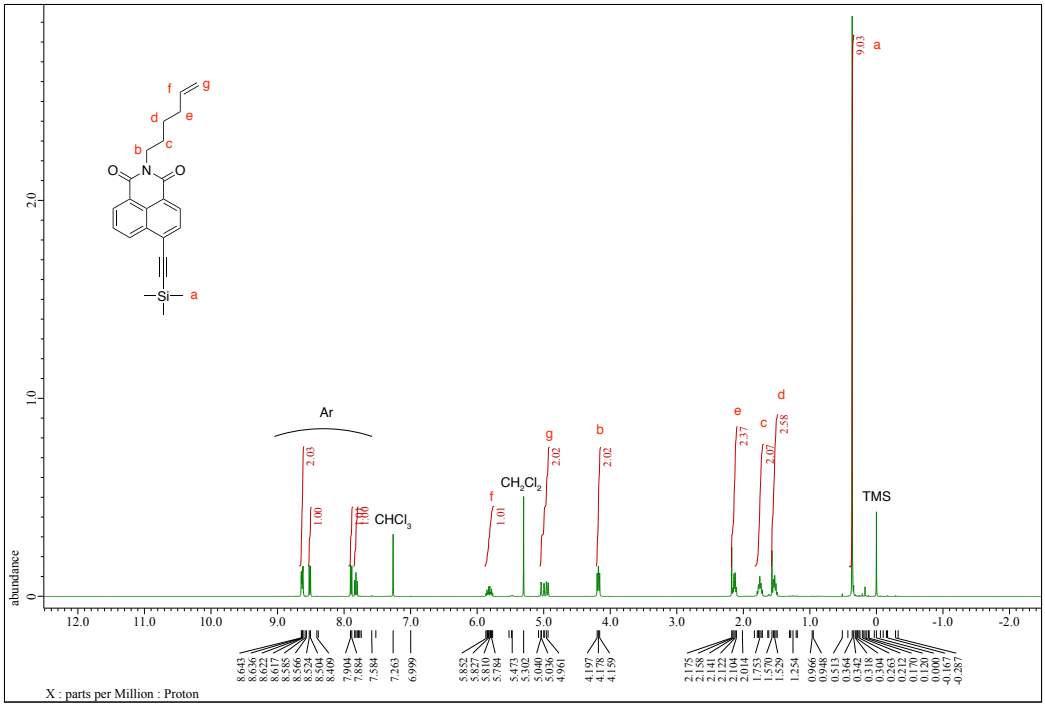

Fig. S5 ^{1}H-NMR (400 MHz) spectrum of *N*-(5-hexenyl)-4-[2-(trimethylsilyl)ethynyl]-1,8-naphthalimide measured in $CDCl_3$ with TMS as an internal standard.

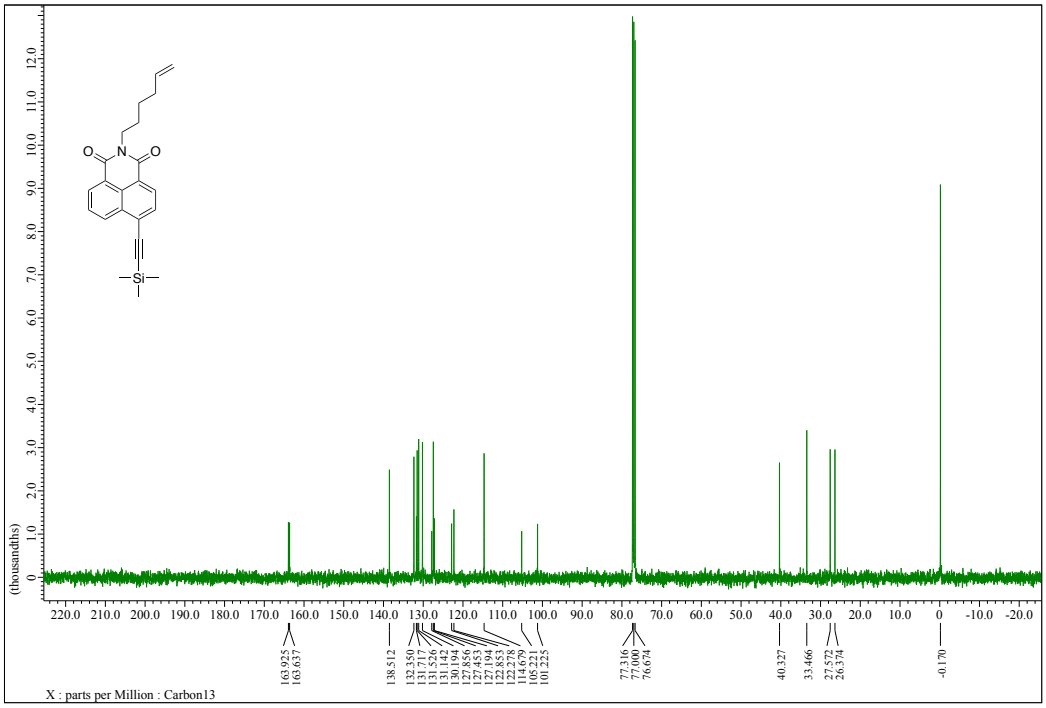

Fig. S6 ^{13}C-NMR (100 MHz) spectrum of *N*-(5-hexenyl)-4-[2-(trimethylsilyl)ethynyl]-1,8-naphthalimide measured in $CDCl_3$.

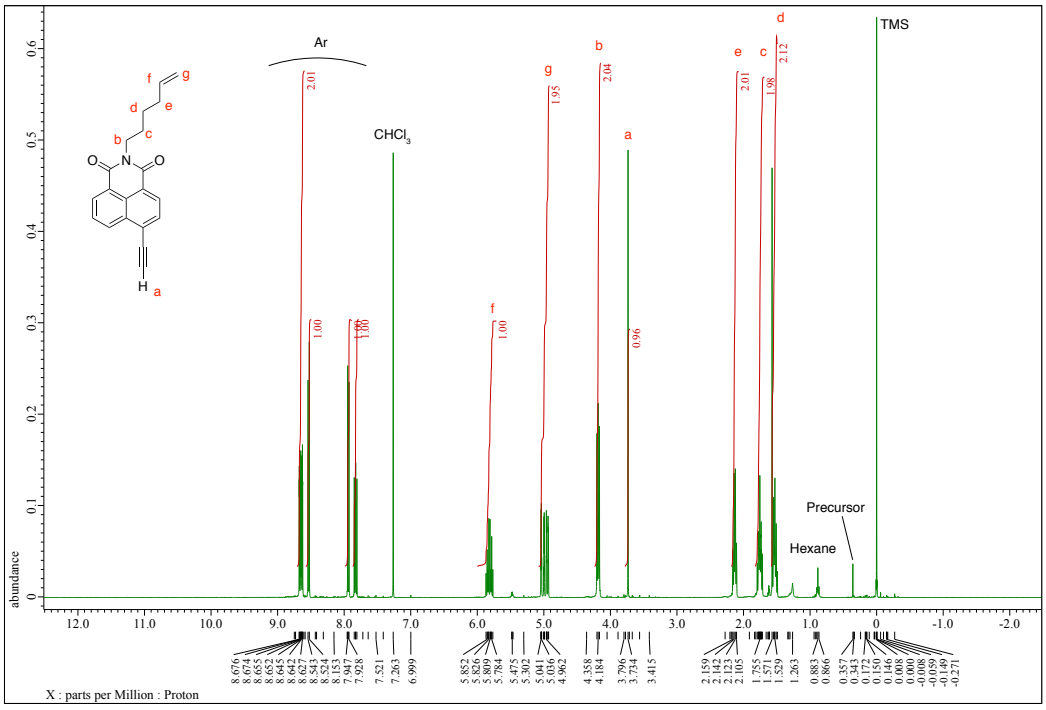

Fig. S7 ^{1}H-NMR (400 MHz) spectrum of *N*-(5-hexenyl)-4-ethynyl-1,8-naphthalimide measured in $CDCl_3$ with TMS as an internal standard.

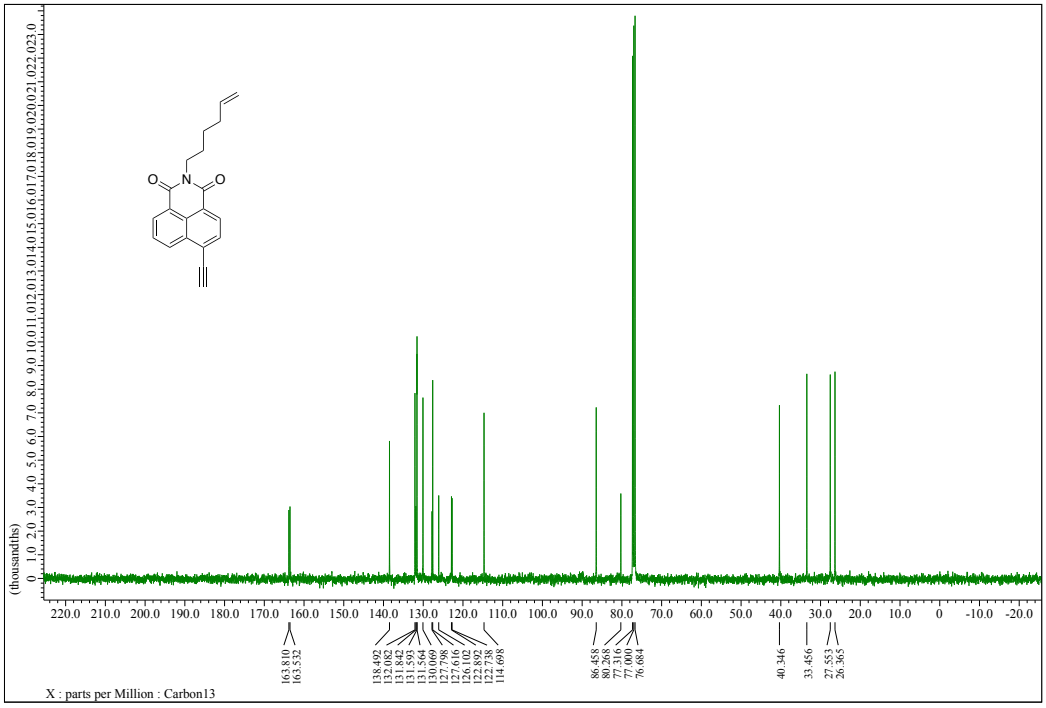

Fig. S8 ^{13}C-NMR (100 MHz) spectrum of *N*-(5-hexenyl)-4-ethynyl-1,8-naphthalimide measured in $CDCl_3$.

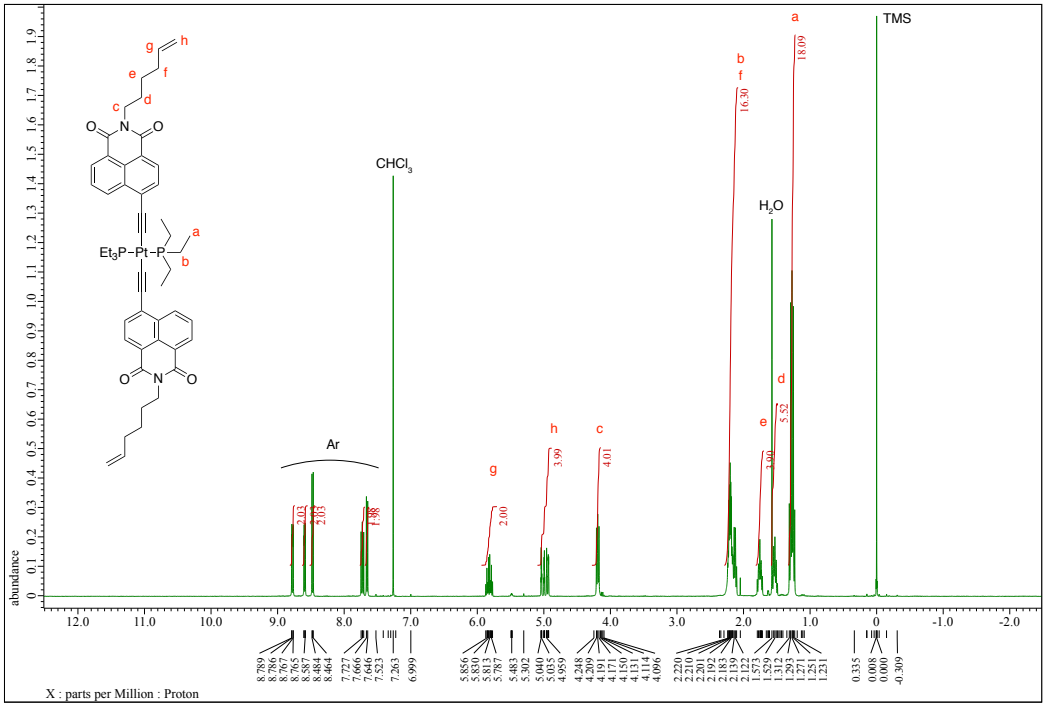

Fig. S9 ^{1}H-NMR (400 MHz) spectrum of **1** measured in $CDCl_3$ with TMS as an internal standard.

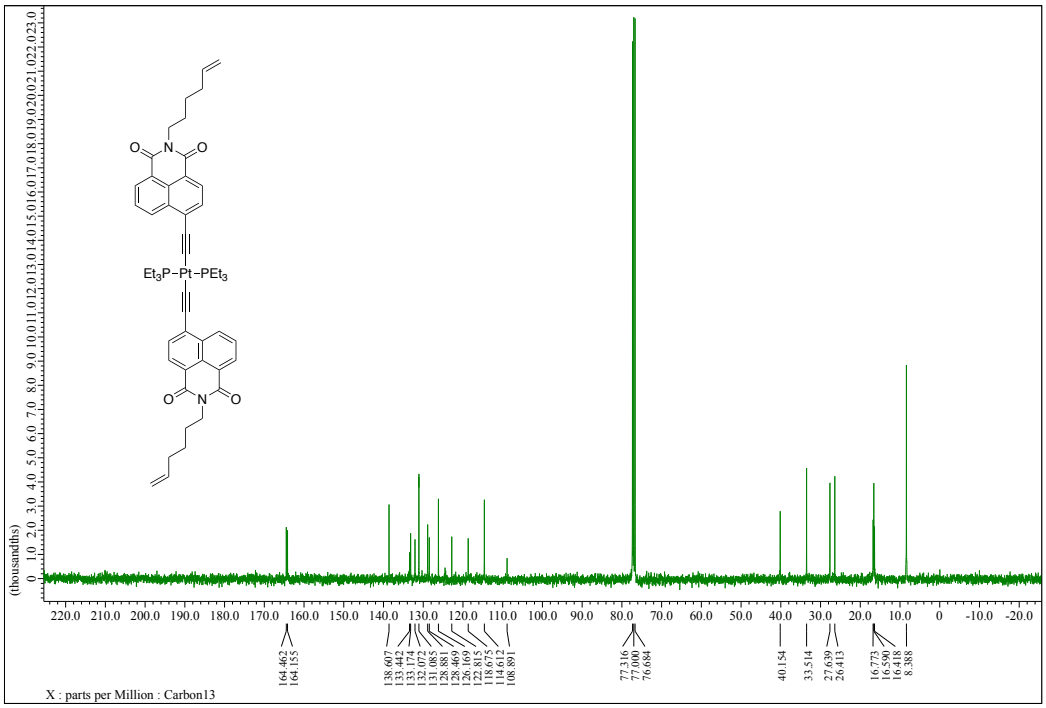

Fig. S10 ^{13}C-NMR (100 MHz) spectrum of **1** measured in $CDCl_3$.

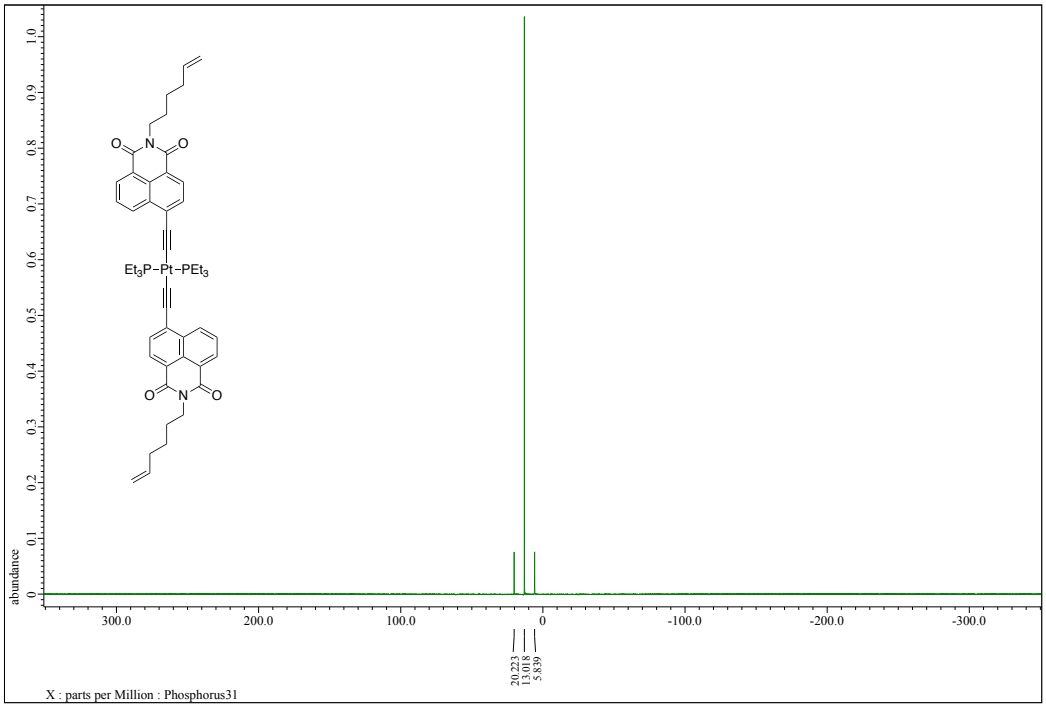

Fig. S11 ^{31}P-NMR (162 MHz) spectrum of **1** measured in $CDCl_3$.

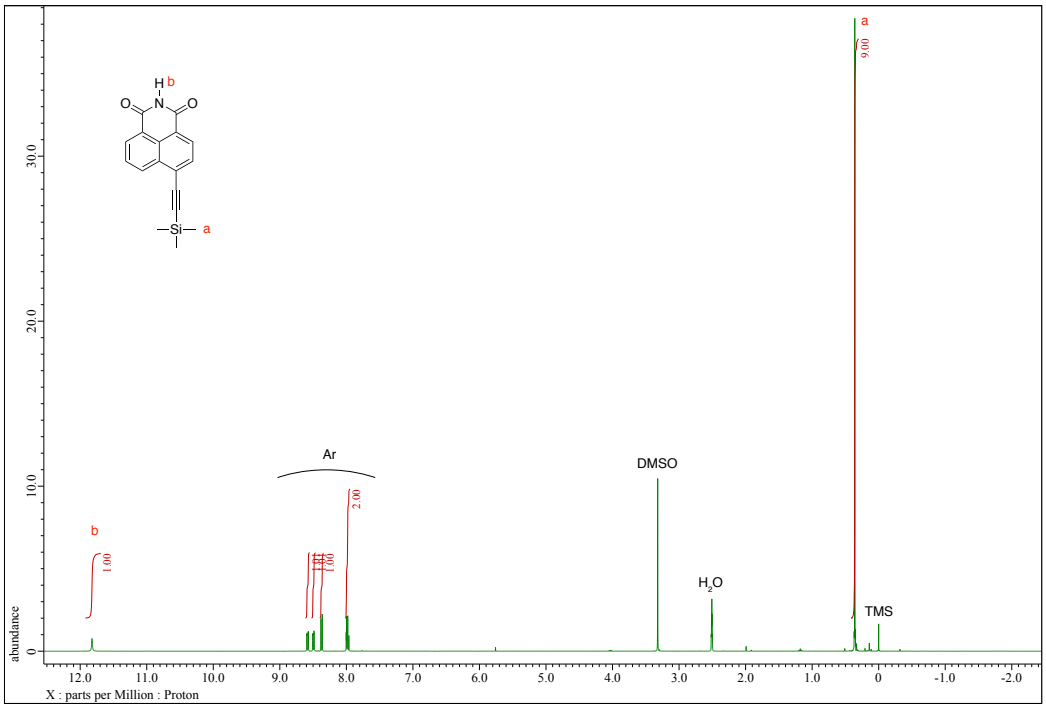

Fig. S12 ^{1}H-NMR (400 MHz) spectrum of 4-[2-(trimethylsilyl)ethynyl]-1,8-naphthalimide measured in DMSO-d_6 with TMS as an internal standard.

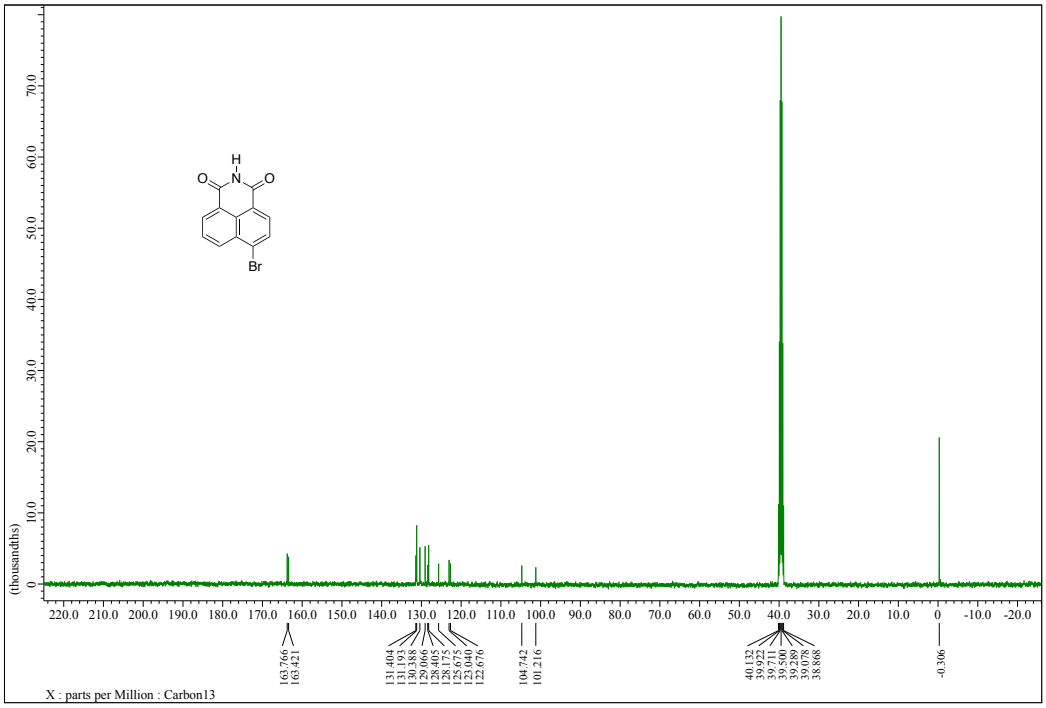

Fig. S13 ^{13}C-NMR (100 MHz) spectrum of 4-[2-(trimethylsilyl)ethynyl]-1,8-naphthalimide measured in DMSO-d_6.

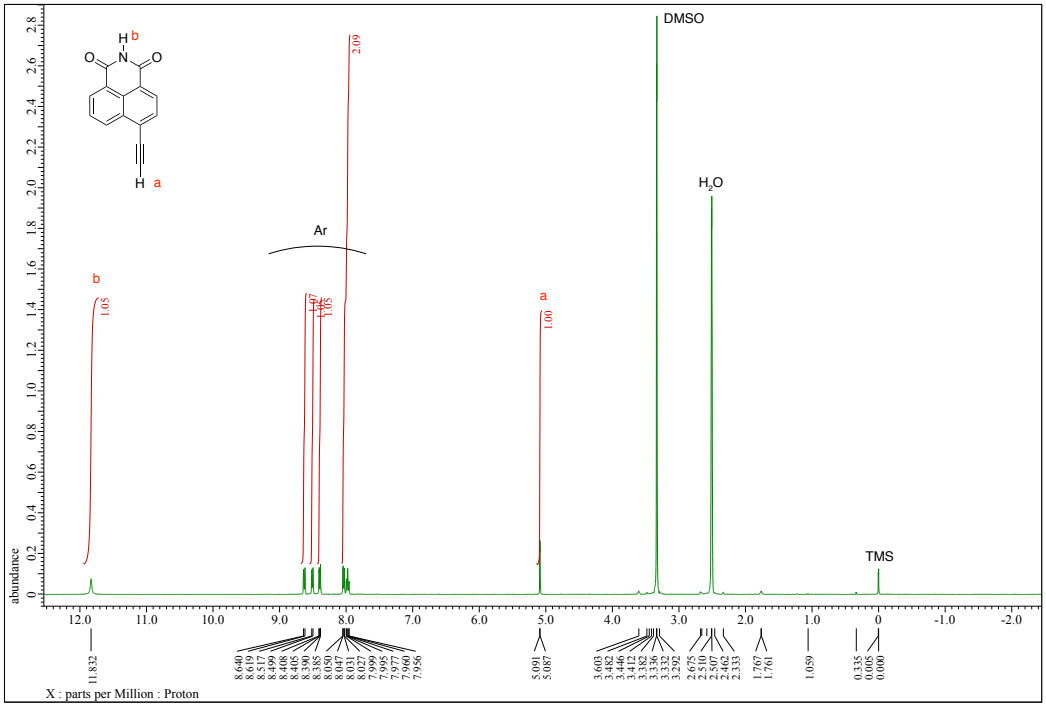

Fig. S14 ^{1}H-NMR (400 MHz) spectrum of 4-ethynyl-1,8-naphthalimide measured in DMSO-d_6 with TMS as an internal standard.

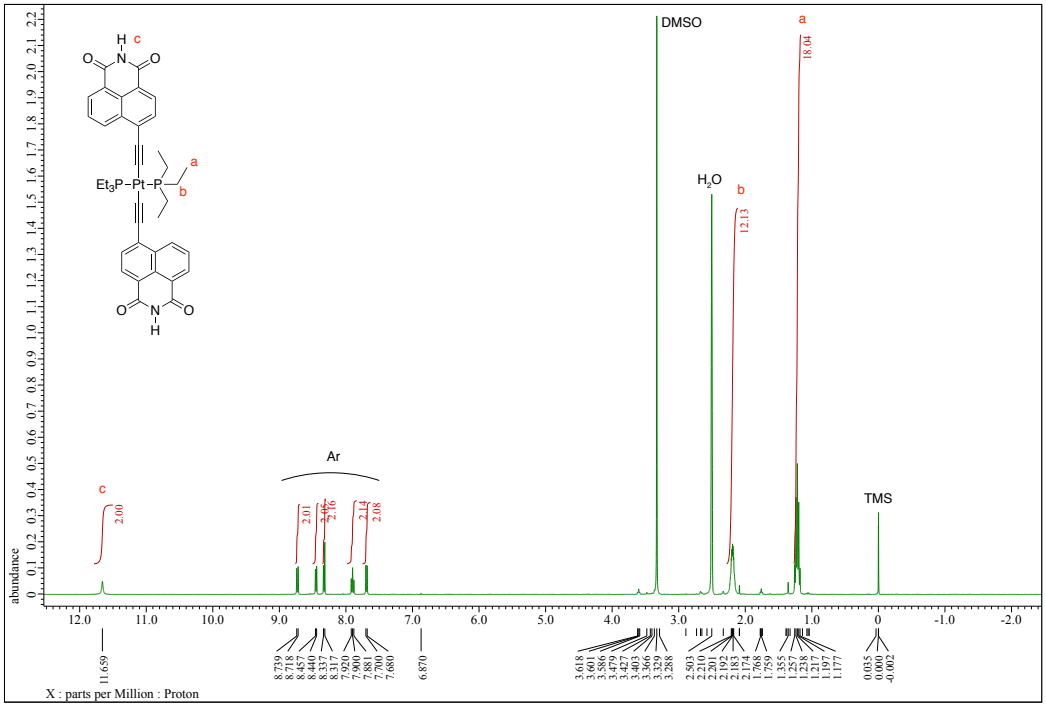

Fig. S15 ^{1}H-NMR (400 MHz) spectrum of **2** measured in DMSO-d_6 with TMS as an internal standard.

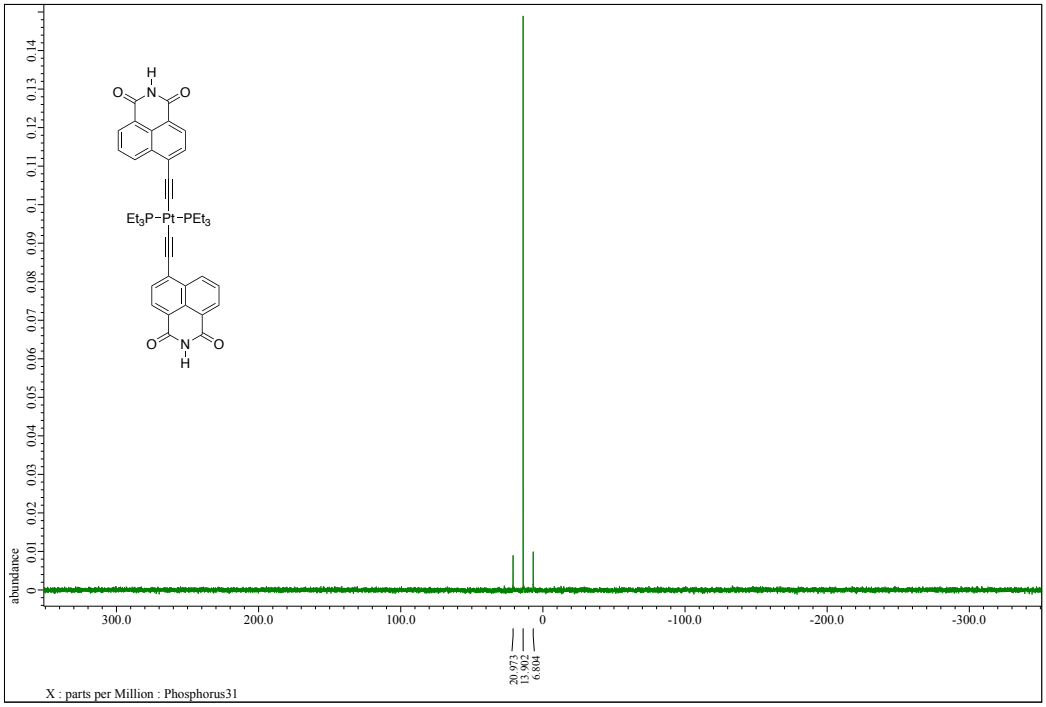

Fig. S16 ^{31}P-NMR (162 MHz) spectrum of **2** measured in DMSO-d_6.

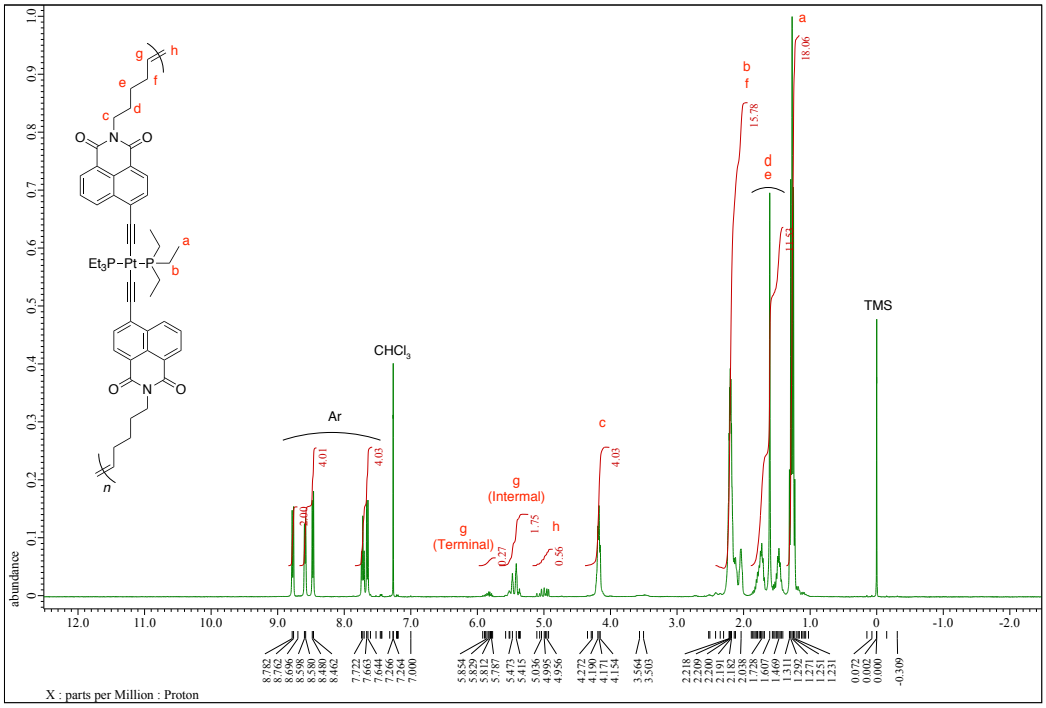

Fig. S17 ^{1}H-NMR (400 MHz) spectrum of oligo(**1**) measured in $CDCl_3$ with TMS as an internal standard.

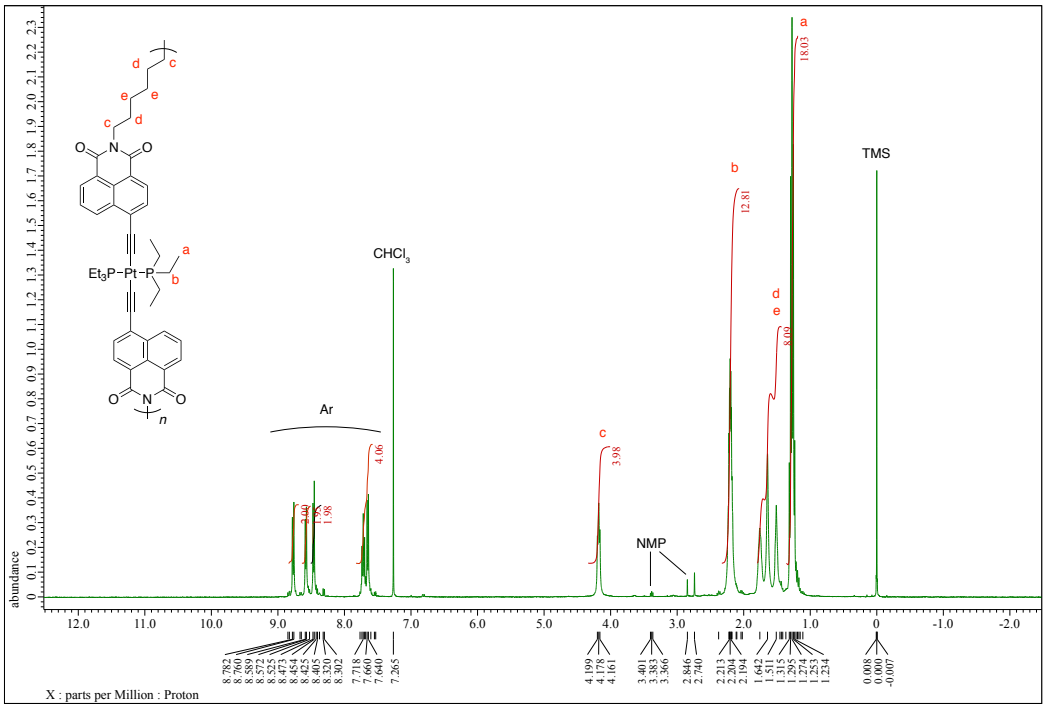

Fig. S18 ^{1}H-NMR (400 MHz) spectrum of oligo(**2-3a**) measured in $CDCl_3$ with TMS as an internal standard.

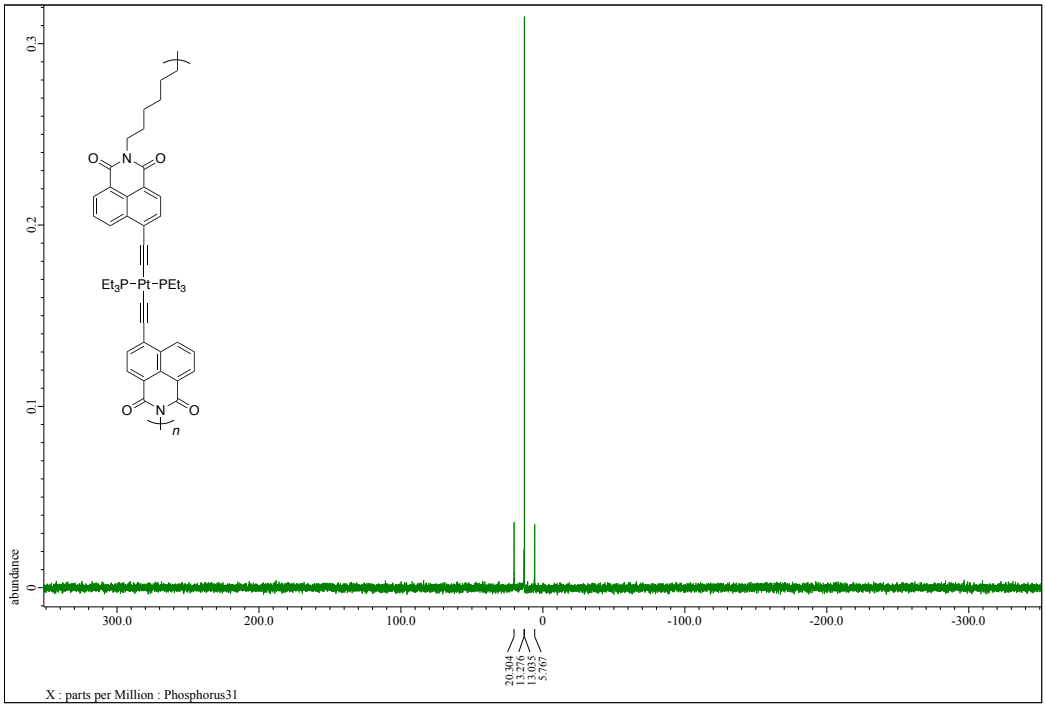

Fig. S19 ^{31}P-NMR (162 MHz) spectrum of oligo(**2-3a**) measured in $CDCl_3$.

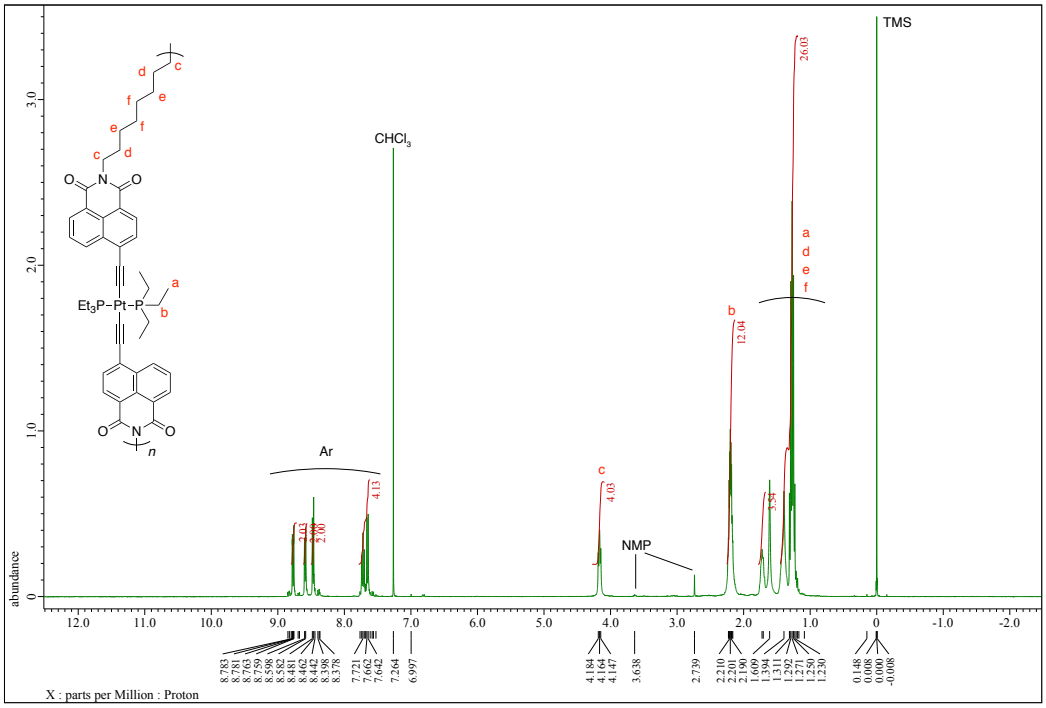

Fig. S20 ^{1}H-NMR (400 MHz) spectrum of oligo(**2-3b**) measured in $CDCl_3$ with TMS as an internal standard.

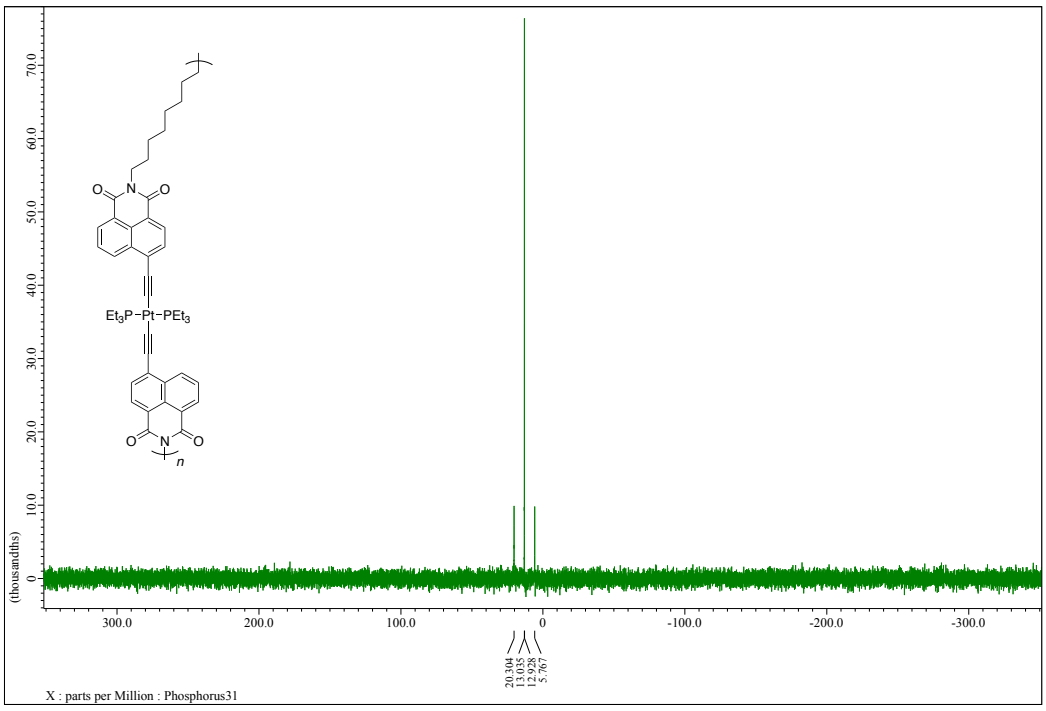

Fig. S21 ^{31}P-NMR (162 MHz) spectrum of oligo(**2-3b**) measured in $CDCl_3$.

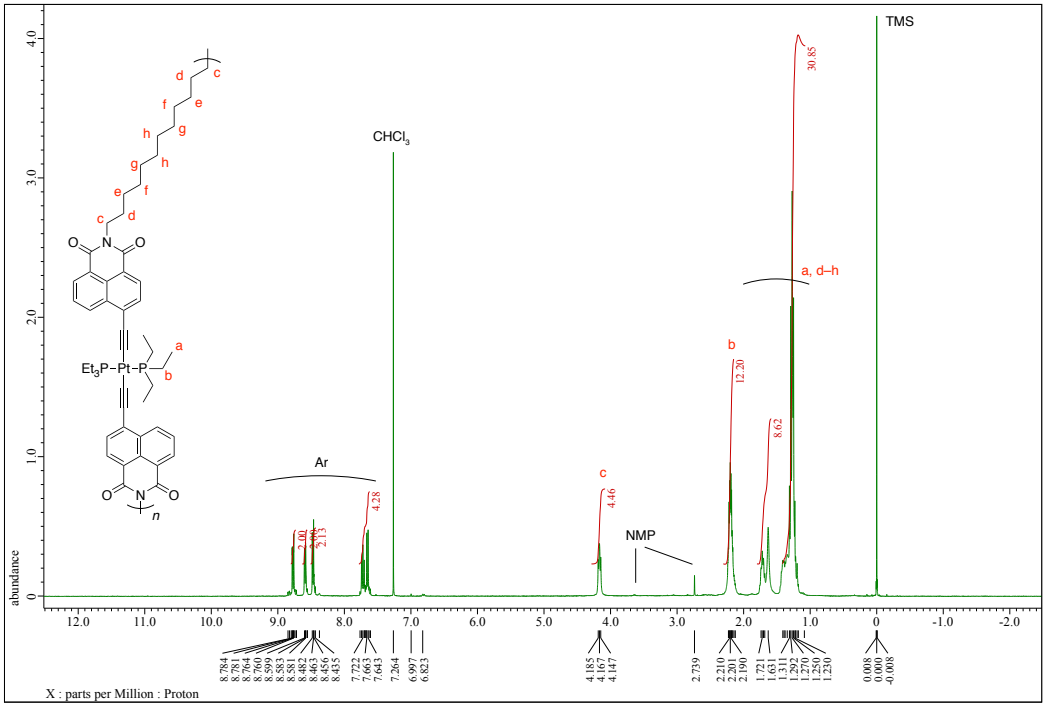

Fig. S22 ^{1}H-NMR (400 MHz) spectrum of oligo(**2-3c**) measured in $CDCl_3$ with TMS as an internal standard.

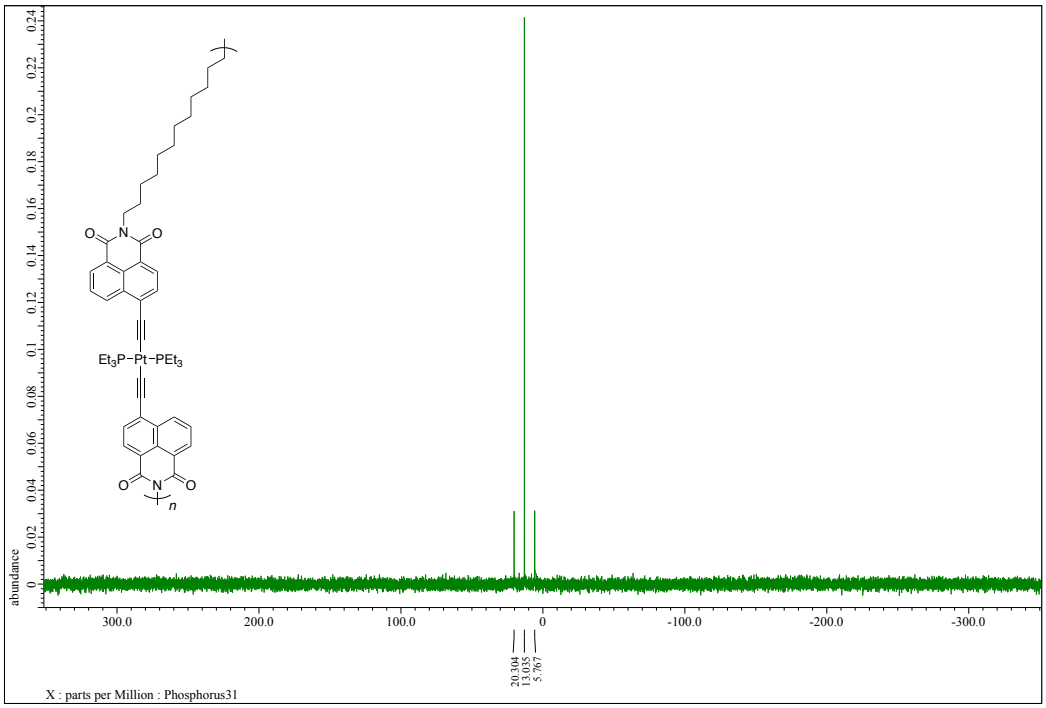

Fig. S23 ^{31}P-NMR (162 MHz) spectrum of oligo(**2-3c**) measured in $CDCl_3$.

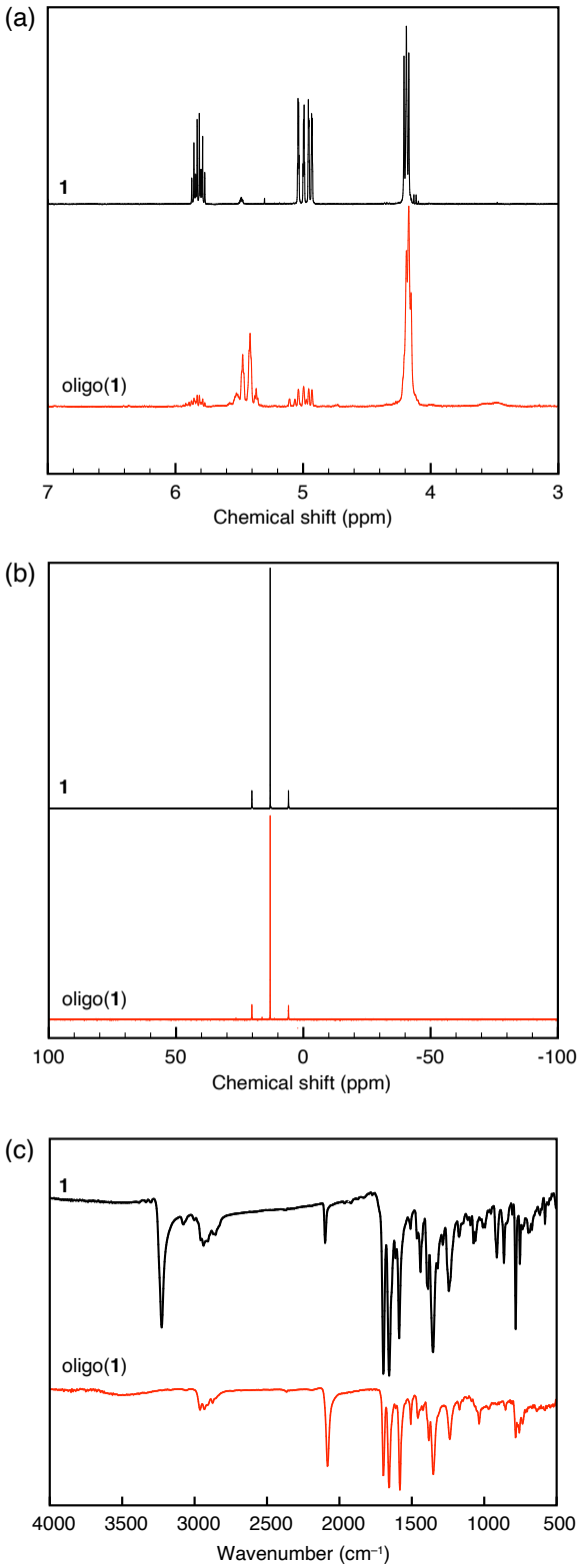

Fig. S24 (a) Partial ^{1}H (400 MHz) and (b) ^{31}P-NMR (162 MHz) spectra of **1** and oligo(**1**) measured in $CDCl_3$, and (c) their IR absorption spectra measured by the KBr pellet method.

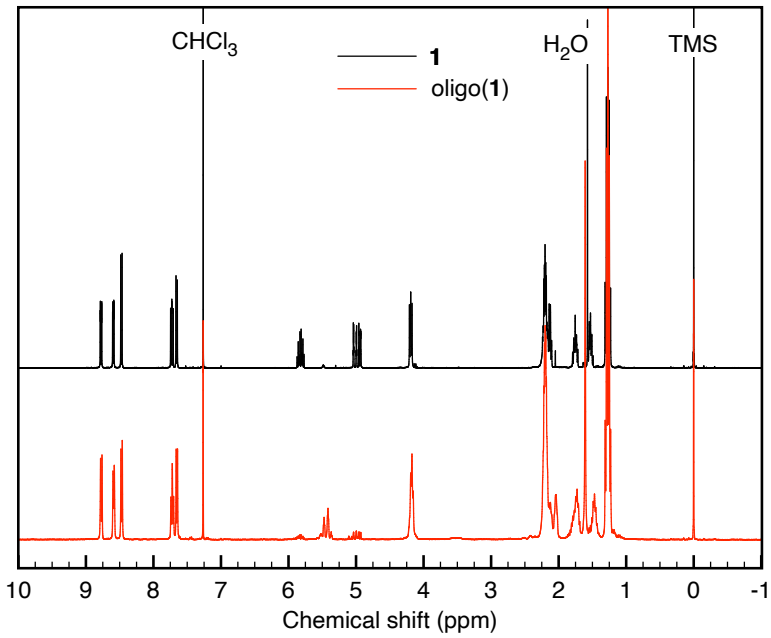

Fig. S25 ^{1}H-NMR (400 MHz) spectra of **1** and oligo(**1**) measured in $CDCl_3$ with TMS as an internal standard.

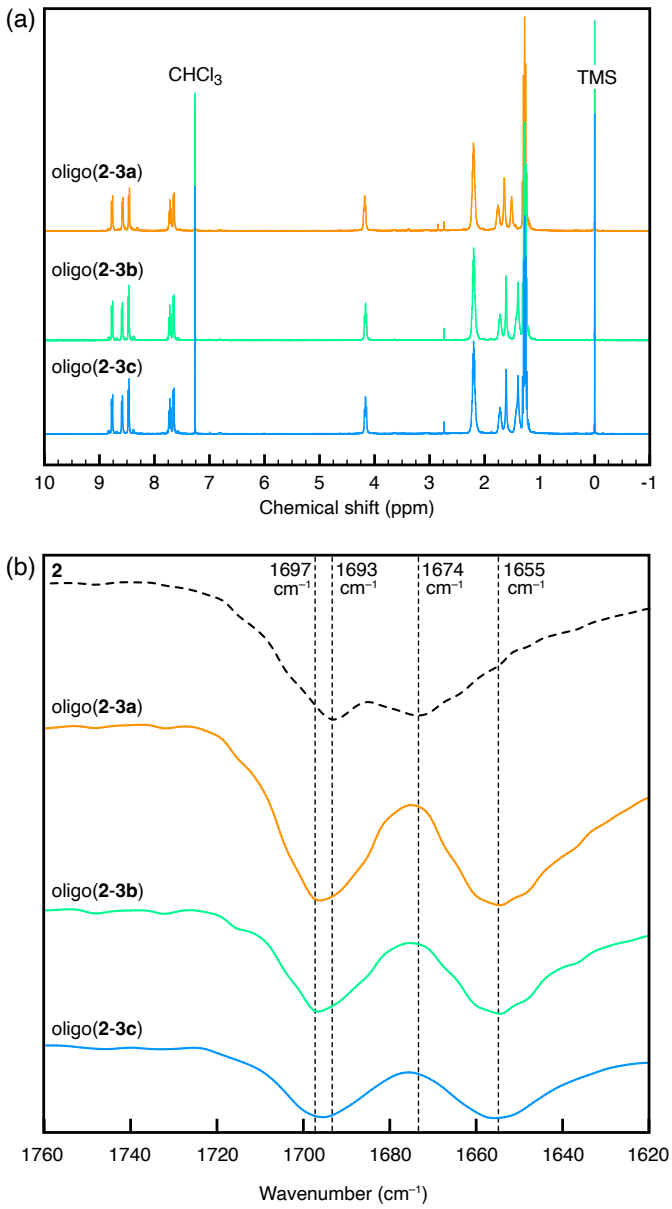

Fig. S26 (a) ^{1}H-NMR spectra of oligo(**2-3a**)–oligo(**2-3c**) measured with TMS as an internal standard in $CDCl_3$, and (b) IR absorption spectra of **2** and oligo(**2-3a**)–oligo(**2-3c**) measured by the KBr method.

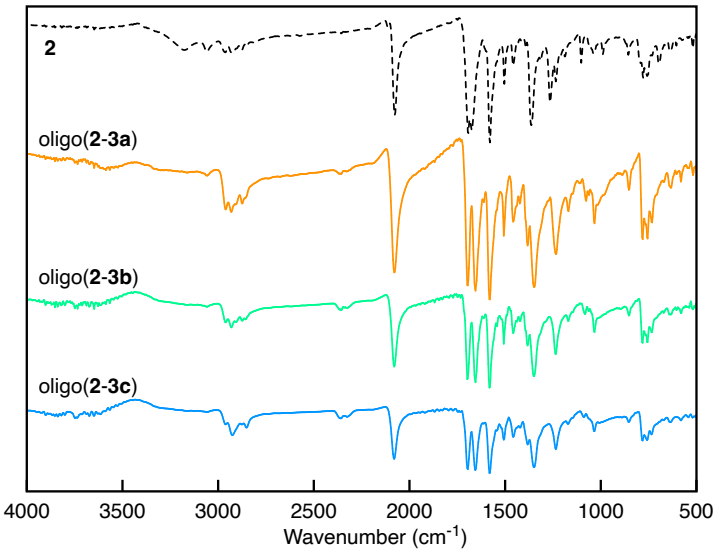

Fig. S27 IR (KBr) absorption spectra of **2** and oligo(**2-3a**)–oligo(**2-3c**).

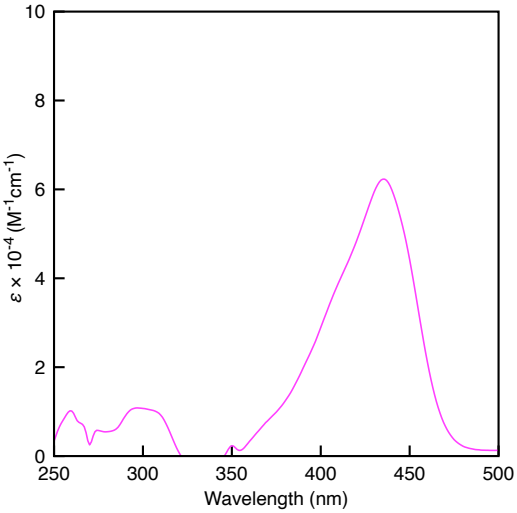

Fig. S28 UV–vis absorption spectrum of **1** measured in $CHCl_3$ (c = 3.0 μM).

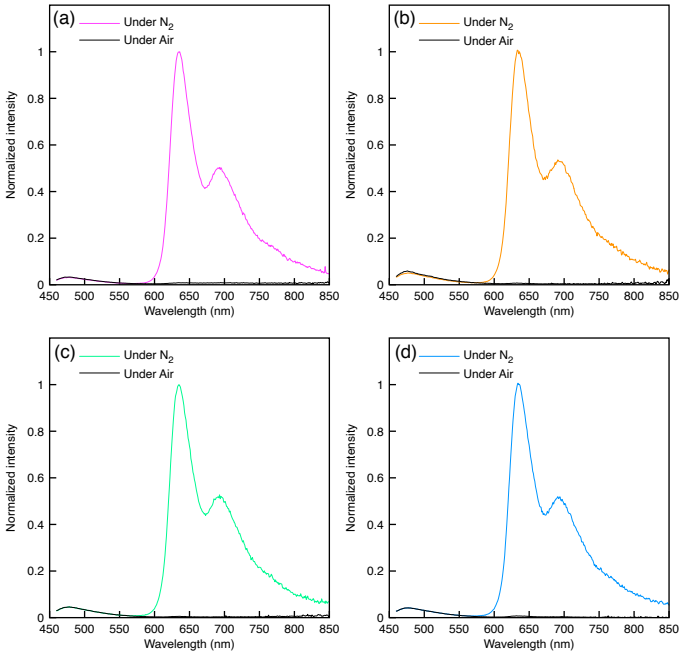

Fig. S29 Photoluminescence spectra of (a) **1**, (b) oligo(**2-3a**), (c) oligo(**2-3b**) and (d) oligo(**2-3c**) measured in $CHCl_3$ (c = 1.5 μM) excited at 440 nm. The intensity was normalized at 635 nm.

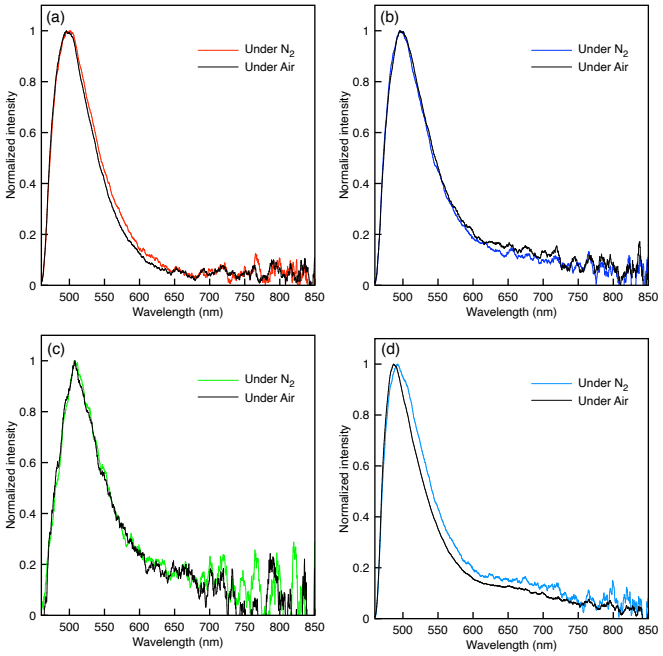

Fig. S30 Photoluminescence spectra of drop-casted films of (a) oligo(**1**), (b) oligo(**2**-**3a**), (c) oligo(**2**-**3b**) and (d) oligo(**2**-**3c**) excited at 450 nm. The intensities were normalized at 495 nm.

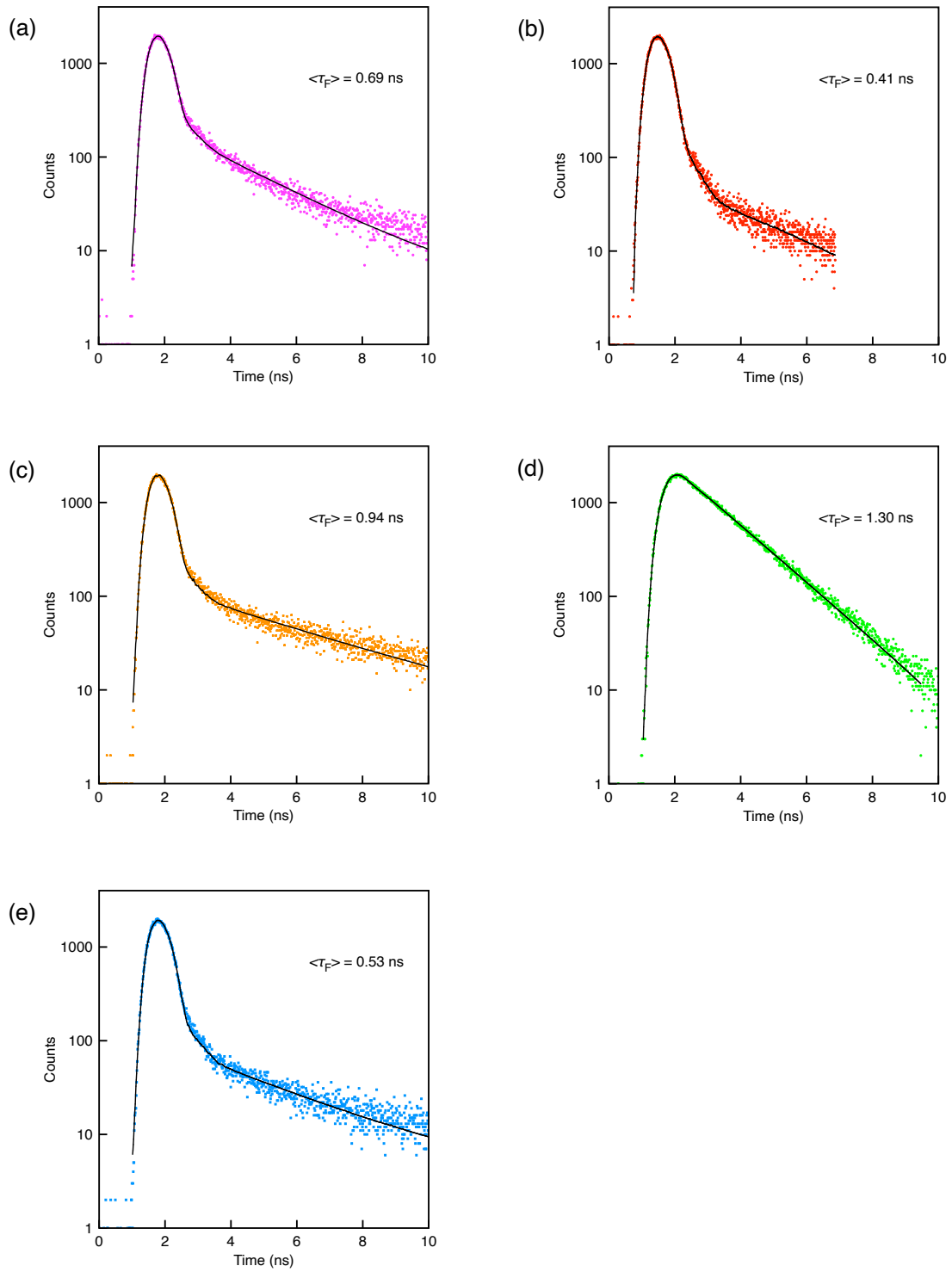

Fig. S31 Fluorescence decay curves of (a) **1** (τ_F = 0.69 ns), (b) oligo(**1**) (τ_F = 0.41 ns), (c) oligo(**2**-**3a**) (τ_F = 0.94 ns), (d) oligo(**2**-**3b**) (τ_F = 1.30 ns) and (e) oligo(**2**-**3c**) (τ_F = 0.53 ns) excited at 405 nm monitored at 480 nm measured in $CHCl_3$ (c = 1.5 μM) under N_2.

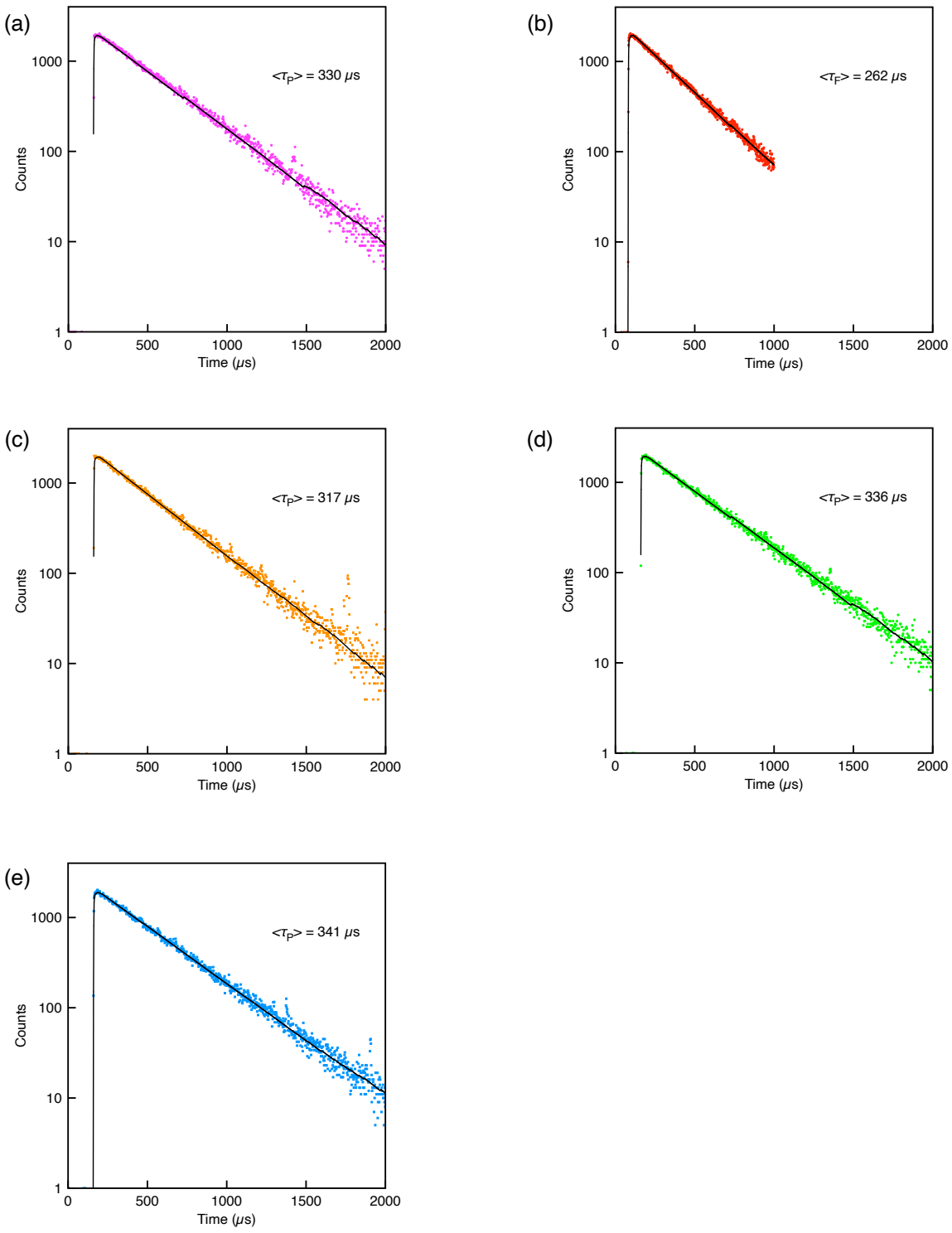

Fig. S32 Phosphorescence decay curves of (a) **1** (τ_P = 330 μs), (b) oligo(**1**) (τ_P = 262 μs), (c) oligo(**2**-**3a**) (τ_P = 317 μs), (d) oligo(**2**-**3b**) (τ_P = 336 μs) and (e) oligo(**2**-**3c**) (τ_P = 341 μs) excited at 450 nm monitored at 640 nm measured in $CHCl_3$ (c = 1.5 μM) under N_2.

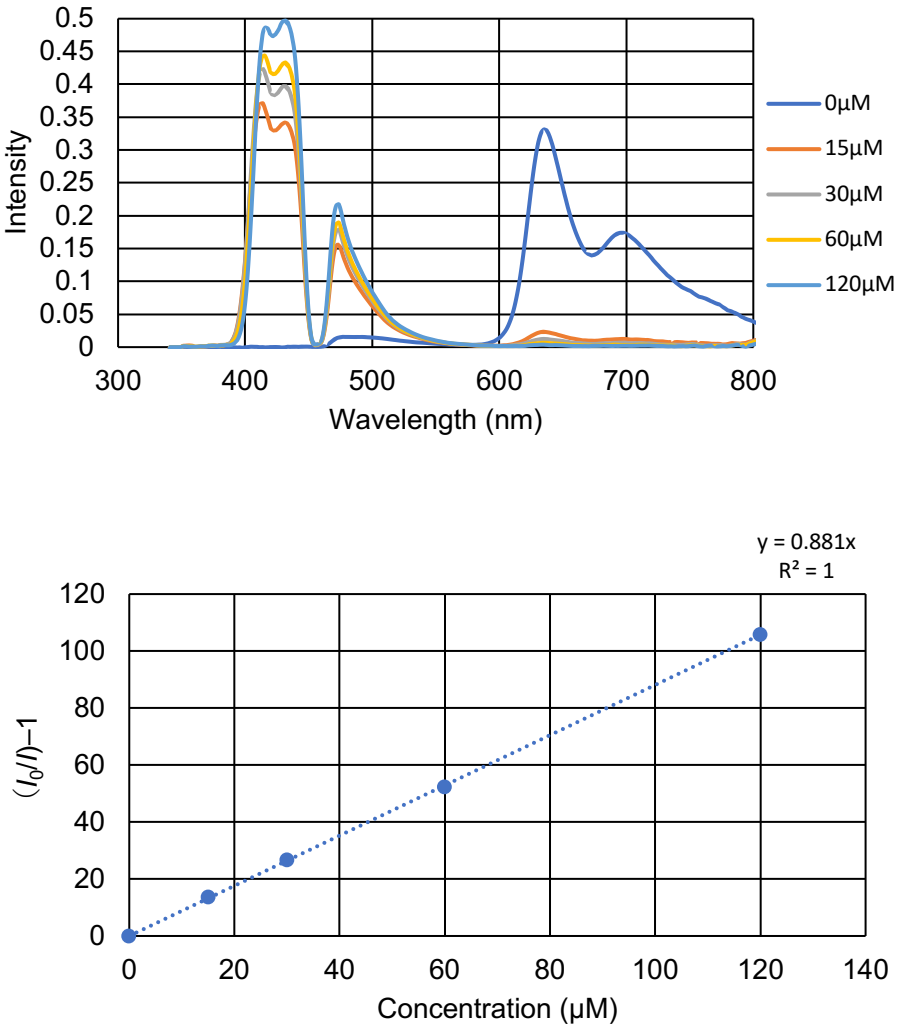

Fig. S33.1 Emission spectra of **1** measured in $CHCl_3$ at various concentrations in the presence of DPA excited at 450 nm under N_2, and the Stern-Volmer plots at 640 nm. The concentration of **1** was 5 μM, and those of DPA were 0, 15, 30, 60 and 120 μM.

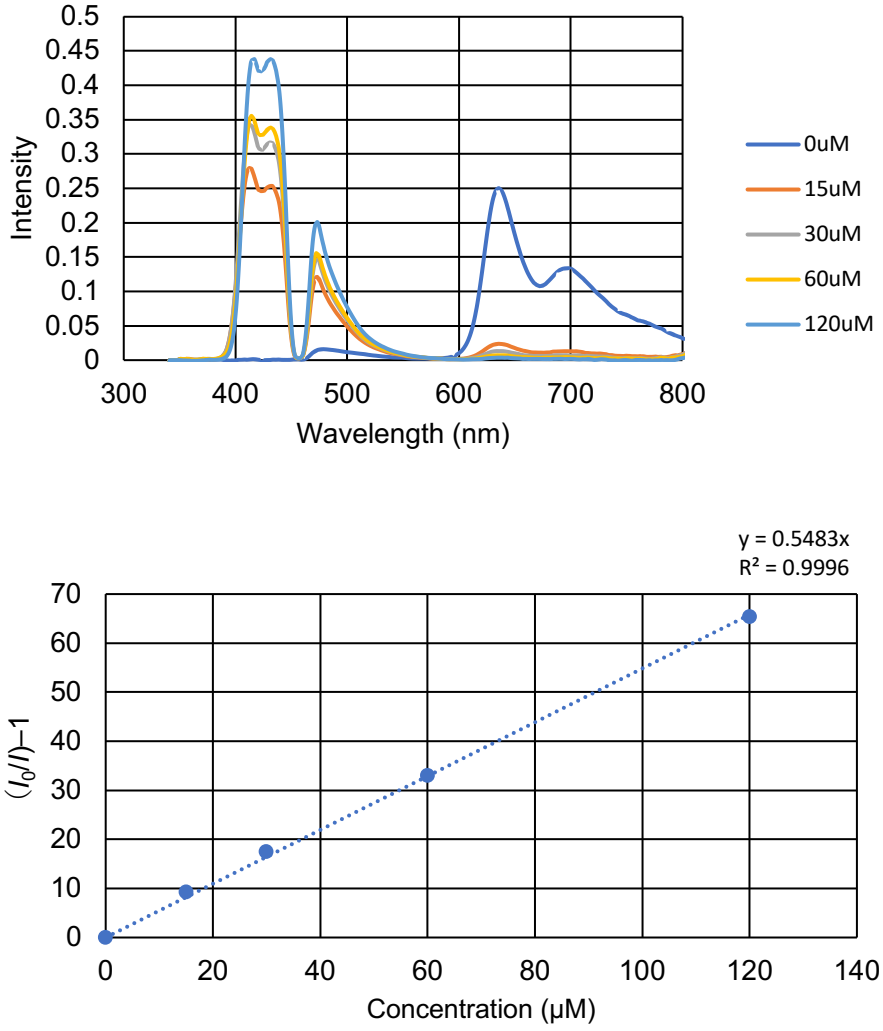

Fig. S33.2 Emission spectra of oligo(**1**) measured in $CHCl_3$ at various concentrations in the presence of DPA excited at 450 nm under N_2, and the Stern-Volmer plots at 640 nm. The concentration of oligo(**1**) was 5 μM, and those of DPA were 0, 15, 30, 60 and 120 μM.

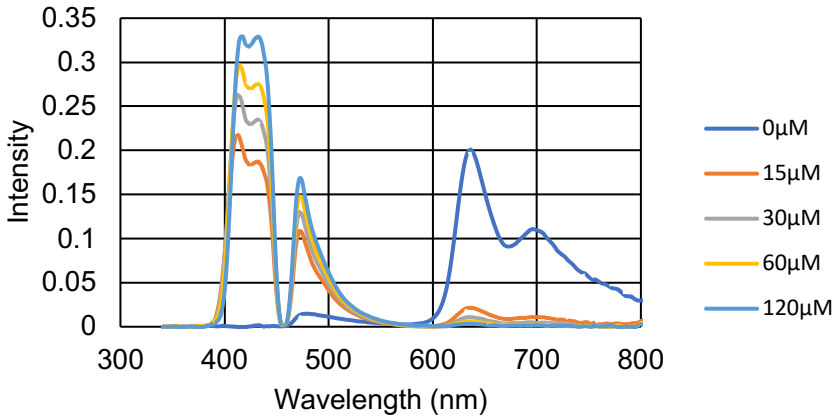

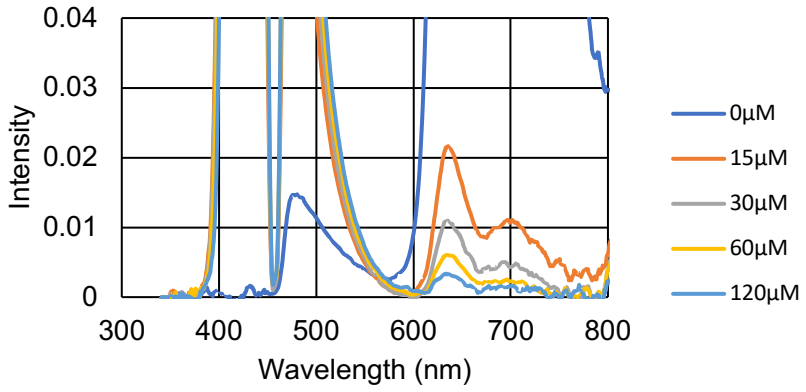

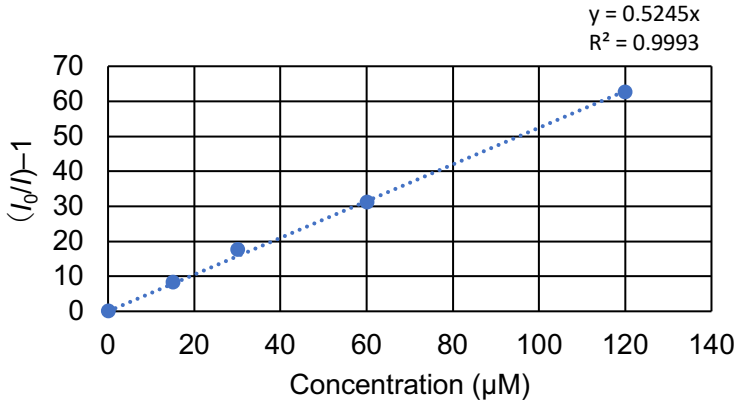

Fig. S33.3 Emission spectra of oligo(**2**-**3a**) measured in $CHCl_3$ at various concentrations in the presence of DPA excited at 450 nm under N_2, and the Stern-Volmer plots at 640 nm. The concentration of oligo(**2**-**3a**) was 5 μM, and those of DPA were 0, 15, 30, 60 and 120 μM.

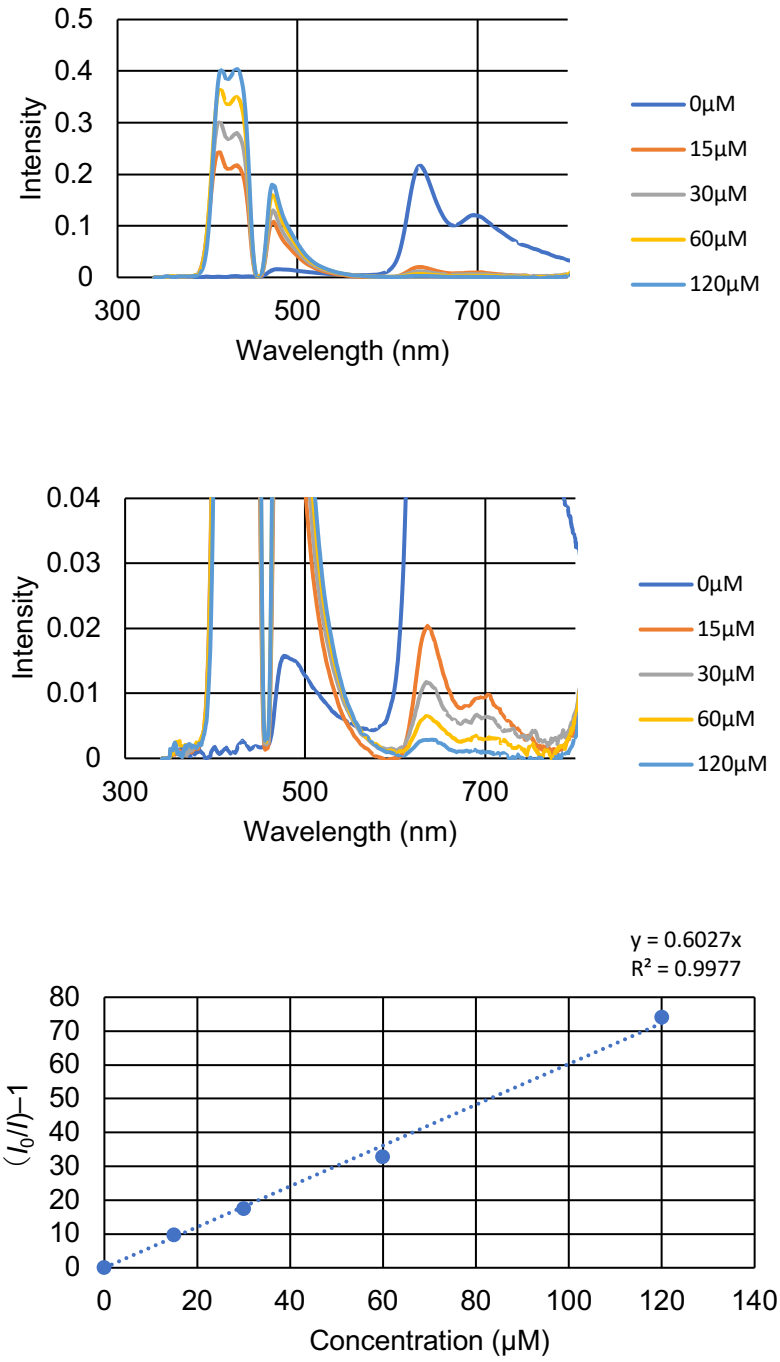

Fig. S33.4 Emission spectra of oligo(**2-3b**) measured in $CHCl_3$ at various concentrations in the presence of DPA excited at 450 nm under N_2, and the Stern-Volmer plots at 640 nm. The concentration of oligo(**2-3b**) was 5 μM, and those of DPA were 0, 15, 30, 60 and 120 μM.

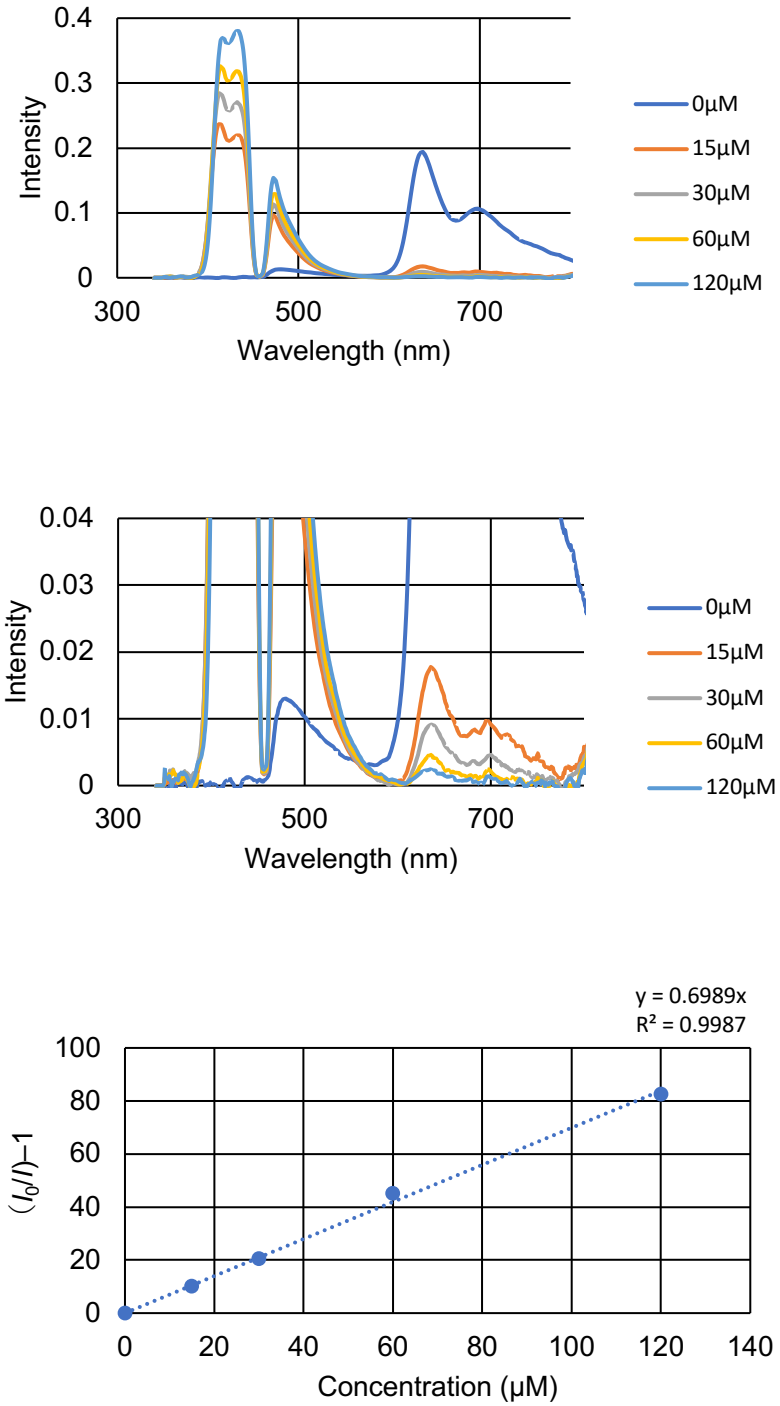

Fig. S33.5 Emission spectra of oligo(**2-3c**) measured in $CHCl_3$ at various concentrations in the presence of DPA excited at 450 nm under N_2, and the Stern-Volmer plots at 640 nm. The concentration of oligo(**2-3c**) was 5 μM, and those of DPA were 0, 15, 30, 60 and 120 μM.

Simulated IR absorptions

The IR absorption spectra of N–H and N–C_3H_7 models (Fig. S26) were simulated by DFT method using the ωB97XD functional and 6-31G* (C, H, N, O, P)-LANL2DZ (Pt) basis set to get information of IR absorptions assignable to two C=O stretching vibrations of cyclic imide moieties of **2** (Table S1). Prior to vibration calculation, the geometries were fully optimized using the same functional and basis set considering the effect of harmonic approximation.

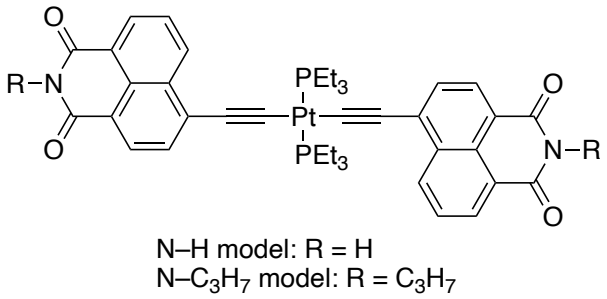

Fig. S34. Chemical structures of N–H and N–C_3H_7 models.

Table S1 IR absorptions of model compounds simulated by DFT method

Compound	C=O stretching vibration (cm^{-1})	
	Symmetrical	Unsymmetrical
N–H model	1845	1841
N–C_3H_7 model	1830	1795

Thermal properties

The thermal stability of oligo(**1**) and oligo(**2-3a**)–oligo(**2-3c**) were analyzed by TGA and DSC as shown in Fig. S35 and listed in Table S2, respectively. All the oligomers did not lose weights at 50–300 °C. The 5% weight loss temperatures of oligo(**2-3a**)–oligo(**2-3c**) were 349–353 °C, which were higher than that of oligo(**1**) (338 °C). The weight residues at 500 °C of oligo(**2-3a**)–oligo(**2-3c**) were 79–81%, higher than that of oligo(**1**) (74%). The order of glass transition temperatures (T_g) was oligo(**1**) ≈ oligo(**2-3c**) < oligo(**2-3b**) < oligo(**2-3a**), which coincided with the chain length between Pt–acetylide complex moieties. Apparently, the presence of internal double bonds also affects the crystallinity,[S4–S6] closely related with thermal properties.

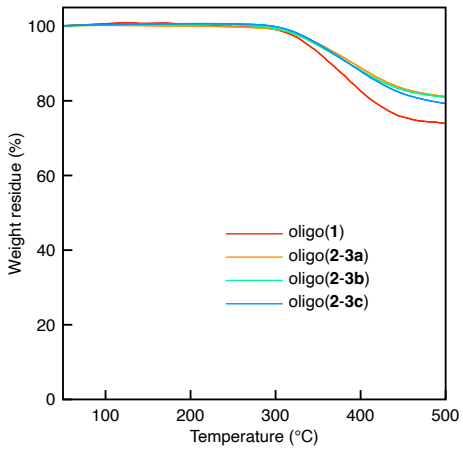

Fig. S35 TGA traces of oligo(**1**) and oligo(**2-3a**)–oligo(**2-3c**) measured at a heating rate = 10 °C/min under N_2.

Table S2 TGA and DSC data of oligo(**1**) and oligo(**2-3a**)–oligo(**2-3c**)

Oligomer	T_{d5} [a] (°C)	$W_{500\,°C}$ [b] (%)	T_g [c] (°C)
Oligo(**1**)	338	74	116
Oligo(**2-3a**)	353	81	182
Oligo(**2-3b**)	349	80	176
Oligo(**2-3c**)	351	79	119

[a] 5% weight loss temperature. [b] Weight residue at 500 °C. [c] Glass transition temperature.

References

S1) Y. Zhou, F. N. Castellano, T. W. Schmidt and K. Hanson, *ACS Energy. Lett*., 2020, **5**, 2322–2326. DOI: 10.1021/acsenergylett.0c01150

S2) M. Verma, V. Luxami and K. Paul, *RSC Adv*., 2015, **5**, 41803–41813. DOI: 10.1039/C5RA00925A

S3) M. J. Frisch, G. W. Trucks, H. B. Schlegel, G. E. Scuseria, M. A. Robb, J. R. Cheeseman, G. Scalmani, V. Barone, G. A. Petersson, H. Nakatsuji, X. Li, M. Caricato, A. V. Marenich, J. Bloino, B. G. Janesko, R. Gomperts, B. Mennucci, H. P. Hratchian, J. V. Ortiz, A. F. Iz-maylov, J. L. Sonnenberg, D. Williams-Young, F. Ding, F. Lipparini, F. Egidi, J. Goings, B. Peng, A. Petrone, T. Henderson, D. Ranasinghe, V. G. Zakrzewski, J. Gao, N. Rega, G. Zheng, W. Liang, M. Hada, M. Ehara, K. Toyota, R. Fukuda, J. Hasegawa, M. Ishida, T. Nakajima, Y. Honda, O. Kitao, H. Nakai, T. Vreven, K. Throssell, J. A. Montgomery, Jr., J. E. Peralta, F. Ogliaro, M. J. Bearpark, J. J. Heyd, E. N. Brothers, K. N. Kudin, V. N. Staroverov, T. A. Keith, R. Kobayashi, J. Normand, K. Raghavachari, A. P. Rendell, J. C. Burant, S. S. Iyengar, J. Tomasi, M. Cossi, J. M. Millam, M. Klene, C. Adamo, R. Cammi, J. W. Ochterski, R. L. Martin, K. Morokuma, O. Farkas, J. B. Foresman and D. J. Fox, Gaussian, Inc., Wallingford CT, 2016.

S4) J. E. O'Gara, K. B. Wagener and S. F. Hahn, *Makromol. Chem., Rapid Commun.*, 1993, **14**, 657–662. DOI: 10.1002/marc.1993.030141006

S5) E. B. Berda, T. W. Baughman and K. B. Wagener, *J. Polym. Sci., Part A: Polym. Chem.*, 2006, **44**, 4981–4989. DOI: 10.1002/pola.21603

S6) G. Rojas, E. B. Berda and K. B. Wagener, *Polymer*, 2008, **49**, 2985–2995. DOI: 10.1016/j.polymer.2008.03.029